University of Colorado, Boulder
CU Scholar

Civil Engineering Graduate Theses & Dissertations Civil, Environmental, and Architectural Engineering

Spring 1-1-2011

Centrifuge Modeling of the Load Settlement Behavior of Shallow Foundations on Geosynthetic-reinforced Soils

Ibrahim Farag Abaidalla
University of Colorado Boulder, ibrahim.abaidalla@colorado.edu

Follow this and additional works at: https://scholar.colorado.edu/cven_gradetds

 Part of the Geotechnical Engineering Commons

Recommended Citation
Abaidalla, Ibrahim Farag, "Centrifuge Modeling of the Load Settlement Behavior of Shallow Foundations on Geosynthetic-reinforced Soils" (2011). *Civil Engineering Graduate Theses & Dissertations*. 199.
https://scholar.colorado.edu/cven_gradetds/199

This Thesis is brought to you for free and open access by Civil, Environmental, and Architectural Engineering at CU Scholar. It has been accepted for inclusion in Civil Engineering Graduate Theses & Dissertations by an authorized administrator of CU Scholar. For more information, please contact cuscholaradmin@colorado.edu.

CENTRIFUGE MODELING OF THE LOAD SETTLEMENT BEHAVIOR OF SHALLOW FOUNDATIONS ON GEOSYNTHETIC-REINFORCED SOILS

By

IBRAHIM ABAIDALLA

B.A., Omar Al-Mukhtar University, Al Bayda, Libya, 2001

A thesis submitted to the

Faculty of the Graduate School of the

University of Colorado in fulfillment

of the requirement for the degree of

Master of Science

Department of Civil, Environmental, and Architectural Engineering

2011

This thesis entitled:

Centrifuge Modeling of the Load Settlement Behavior of Shallow Foundations on Geosynthetic-Reinforced Soils

written by Ibrahim Abaidalla

has been approved for the Department of Civil, Environmental, and Architectural Engineering

_____

(John Scott McCartney)

_____

(Hon-Yim Ko)

_____

(Dobroslav Znidarcic)

Date_____

The final copy of this thesis has been examined by the signatories, and we Find that both the content and the form meet acceptable presentation standards of scholarly work in the above mentioned discipline.

Abaidalla, Ibrahim F. (M.Sc., Civil, Environmental, and Architectural Engineering)

Centrifuge Modeling of the Load Settlement Behavior of Shallow Foundations on Geosynthetic-Reinforced Soils

Thesis directed by Dr. John S. McCartney

Geosynthetic reinforcement of granular fill overlying soft soils is a possible approach to improve the load-settlement behavior of foundations. Geosynthetic reinforcement of granular fill is intended to function by providing lateral restraint to the fill, which reduces the potential for settlement of underlying soils by distributing the foundation load to a wider area. The approach may help avoid high costs associated with other alternatives such as deep foundations or modification of the underlying soil. Further, the use of geosynthetic reinforcement may require less backfill soil to adequately distribute the foundation load to a wider area. In other words, geosynthetic reinforcements are expected to increase the lateral restraint of granular fill, minimizing lateral deformations during application of a surficial foundation load. The objective of this research project is to use small-scale centrifuge tests to evaluate the load-settlement curves of surficial foundations on geosynthetic reinforced sand layers overlying soft material. The variables investigated in this study include the depth and number of geosynthetic layers and the centrifuge acceleration level. It was found that geosynthetic reinforcement only leads to an improvement in the load-settlement curves when the confining pressure is low enough that the pullout resistance of the geosynthetics can be mobilized.

TO

MY PARENTS AND MY FAMILY

ACKNOWLEDGEMENTS

I would like to thank and appreciate Professor John McCartney for his support since the first day that I started at the school and for persevering with me as my advisor throughout the time it took me to complete this research and write my dissertation. This research was one of the most important and formative experiences in my life.

The members of my dissertation committee, Professor Hon-Yim Ko and Professor Dobroslav Znidarcic, have generously given their time and expertise to better my work. I thank them for their contribution and their advices.

My thanks must go to my country, Libya, and Omar Al-Mukhtar University for sending me and supporting me to continue my graduate study at University of Colorado, Boulder. Their support increased my understanding and knowledge of civil engineering materials as well as various other emerging technologies.

I need also to express my gratitude and deep appreciation to my parents, my wife, my brothers and sisters, students in our department, and anyone helped me and supported me even with one word.

Table of Contents

Table of Figures

CHAPTER I

INTRODUCTION

1.1 Motivation

Geosynthetic reinforcement of compacted granular fill overlying soft soils is a possible approach to improve the load-settlement behavior of bearing capacity of foundations (Gabr et al. 2000; Giroud et al. 2004). Geosynthetic reinforcements function by adding tensile resistance and lateral restraint to the compacted granular fill (Ismail and Raymond 1997), leading to a wider area of stress distribution and reduced settlement of underlying soils. This approach is typically used with the goal of avoiding high costs associated with other alternatives such as deep foundations, modification of the foundation soil, or incorporation of additional structural granular fill. Geosynthetic reinforcement may also permit distribution of stresses to a wider area of the soft soil with a thinner layer of granular fill, reducing material costs.

1.2 Research Objectives

The main objective of this study is to evaluate the effect of using geogrid reinforcement to improve the load-settlement behavior of shallow foundations on granular fills overlying a soft layer of soil. Further, a secondary objective is to develop a centrifuge testing module which could be used to evaluate the impact of geosynthetic reinforcement on the bearing capacity of foundations in an instructional centrifuge. Specifically, because the resisting forces of the geosynthetic depend on the self-weight of the overlying soil, the geotechnical centrifuge may be suitable to evaluate the impact of the geosynthetic on the load-settlement behavior may be evaluated in a geotechnical centrifuge. In addition to the technical outcomes of the centrifuge testing program, the outcome of this research will be the setup and procedures for an educational centrifuge module suitable for use in an introduction to geotechnical engineering course.

1.3 Research Approach

The research approach used in this study is to construct laboratory-scale models of soil layers atop a soft subsurface layer, and to measure their load-settlement curves during centrifugation in the instructional centrifuge at the University of Colorado at Boulder. The soft subsurface layer is modeled by styrofoam to decrease preparation time and improve repeatability. In addition to a modeling of models study to evaluate the load-settlement curves of different centrifuge models, the impact of centrifuge acceleration layer on the load-settlement curve of soil layers having geosynthetic reinforcements at different depths as well as multiple geosynthetic layers is investigated. The impact of centrifuge acceleration is useful to assess the impact of particle self-weight on the load-settlement curve of a foundation on a reinforced soil layer.

1.4 Scope of this thesis

A literature review is provided in Chapter 2 to summarize experiments and theory for the bearing capacity of foundations on reinforced soils. The experimental testing program in this study is described in Chapter 3, including the description of the model and the instrumentation. The materials used in this study and their engineering properties are presented in Chapter 4. The test procedures, including preparation of the device, are described in Chapter 5. Results from the series of tests performed in this study are presented in Chapter 6. An elastic analysis of the layered soil profile is presented in Chapter 7 to interpret the results of the tests. The conclusions and recommendations are presented in Chapter 8.

CHAPTER II

LITERATURE REVIEW

2.1 Overview of the Load-Settlement Behavior of Foundations

2.1.1 Load-Settlement Failure Modes

This study involves an evaluation of the load-settlement curves of foundations on geosynthetic reinforced soils. Accordingly, a review of the expected shapes of load-settlement curves for different soils is presented in this section. Bearing capacity failure can be classified to three principal modes, including general shear failure (Caguot, 1934; Buisman, 1935; Terzaghi, 1943), local shear failure (Terzaghi, 1943; De Beer and Vesić, 1958), and punching shear failure (De Beer and Vesić, 1958; Vesić, 1963).

General shear failure is typically observed in dense sands and stiff clays. In stress-controlled loading conditions such as those present in foundations, failure is often observed to be sudden and catastrophic unless the structure prevents the footing from rotating. In strain-controlled loading conditions, for example when the load is transmitted to a foundation by jacking, a visible decrease of load necessary to produce footing movement after failure may be observed (strain softening. The failure surface for general shear failure is well defined, as shown in Figure 2.1.

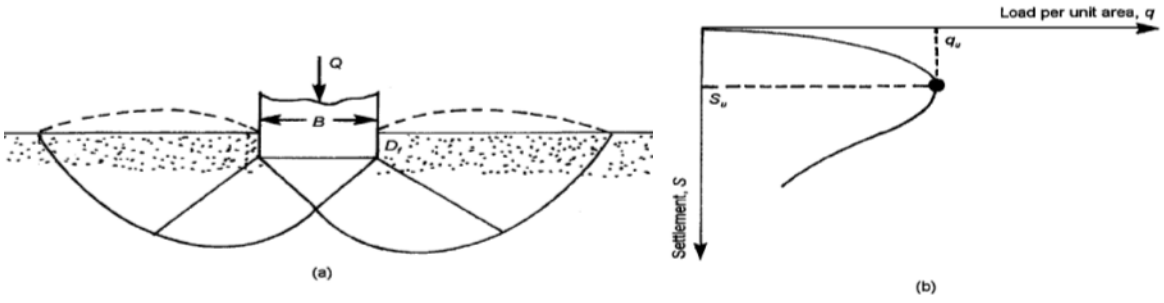

Figure 2.1 General shear failure (Das 1999): (a) Mechanism; (b) Typical load-settlement curve.

Local shear failure is observed where a foundation is supported by medium dense sand or slightly overconsolidated clay. Failure in this situation is not as catastrophic as general shear

failure. From Figure 2.2, the load-settlement curve becomes steeper and erratic as the applied load increases. When the bearing capacity (q) reaches the ultimate value (q_u), the failure surface reaches the ground surface. A peak load is typically not observed in the load-settlement curve for this failure mode.

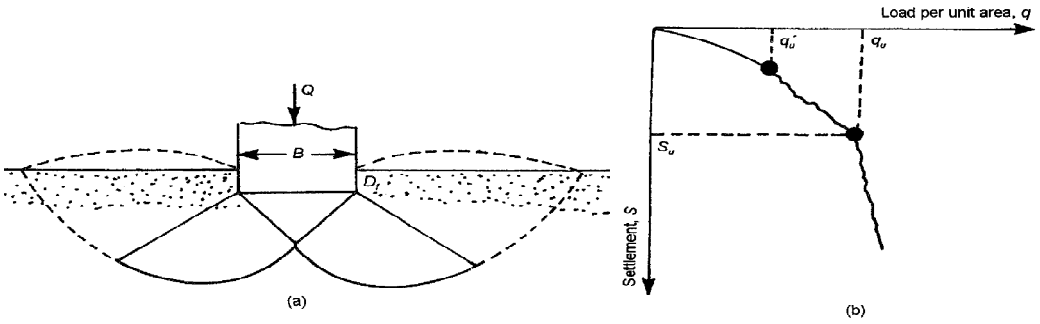

Figure 2.2 Local shear failure (Das 1999): (a) Mechanism; (b) Typical load-settlement curve.

Punching shear failure is noted in foundations on loose sand or soft clayey soil. In this mode, the footing will start penetrate and continue punching the soil as the vertical load increases. Continued penetration of the footing is made possible by vertical shear around the footing perimeter. There is no visible collapse except for sudden small movements of the foundation in the vertical direction. Also, the failure surface does not extend up to the ground surface, as shown in Figure 2.3.

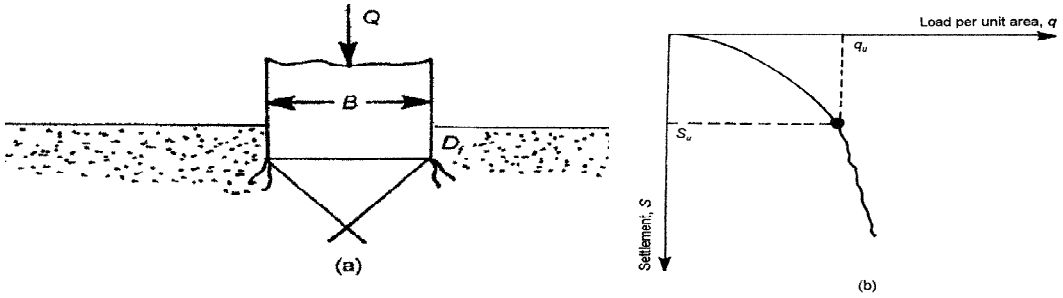

Figure 2.3 Punching shear failure (Das 1999): (a) Mechanism; (b) Typical load-settlement curve.

2.2 Previous Studies on Bearing Capacity of Geosynthetic-Reinforced Soils

Geosynthetics have been used in reinforcement applications since the mid-1970s (Binquet and Lee 1975a, 1975b). These researchers investigated the mechanisms of using reinforced earth slabs to improve the bearing capacity of granular soils. They tested the load-settlement behavior of model strip footings on sand reinforced with wide strips of household aluminum foil. They developed an analytical method for estimating the increased bearing capacity based on their tests. They indicated that both the bearing capacity and settlement can be improved by a factor of 2 to 4 compared to unreinforced sand. This study was followed by many experimental studies on the bearing capacity of footing on reinforced sands, most of which were based on small-scale laboratory tests. The results of previous works indicated that the use of reinforcements can appreciably increase the soil's bearing capacity and reduce the footing settlement. However, the self-weight of the soil can have an important impact on the bearing capacity of soils, so these results under full-scale conditions are uncertain.

Das et al. (1994) constructed two foundation models, one in sand and the other in clay. Each foundation was constructed from aluminum plates measuring 76.2 mm in width by 304.8 mm in length. A rough-base condition was achieved by cementing a thin layer of sand to the bases of the model foundations. Two sand layers were prepared in boxes with internal dimensions of 1.1 m length, 0.3048 m width, 0.91 m depth using dry pluviation. The foundation was tested in plane-strain conditions, so the inside walls of the boxes were polished to reduce friction with the ends of the foundations as much as possible. They used biaxial geogrid as the reinforcement material for all tests. The geogrid layers were placed at the desired depths during pluviation, and the model foundations were placed on the surface of the compacted soil bed. The load and corresponding foundation settlement were measured using a proving ring and two dial gauges.

For the tests on clay, the settlement of the strip foundation at the ultimate load on reinforced and unreinforced case was the same. However, for the tests on sand, an increase in the ultimate load brought about by the reinforcement is accompanied by an increase in the settlement of the foundation. The total depth for the geogrid layers to mobilize the maximum possible ultimate bearing capacity was 2.00B in sand and 1.75B in clay, where B is the footing width. The first layers of the geogrid layer were recommended to be placed at depths of 0.3B to 0.4B to obtain the most improvement.

Gabr and Hart (2000) performed a total of 9 plate load tests on full-scale layers of Ohio river sand. Their tests were performed in a box having dimensions of 1.52 m in length, 1.52 m in width, and 1.37 m in depth. These dimensions were selected based on estimated stress distributions. Two types of biaxial geogrids were utilized in the testing program (SR1 and SR2), where SR1 and SR2 have initial tangent moduli of 205kN/m and 329kN/m, respectively. The top geogrid layer placed at depths (u) of 150, 229, and 300 mm from the bottom of the plate. Three geogrid layers were used, with a vertical spacing between the geogrids of 300 mm. The soil was compacted using a jackhammer with a footing area of 200 mm by 200 mm. Test on unreinforced soil layers were performed to provide a baseline case. The load increments were applied to the test plate using a hydraulic jack with a capacity of 75 kN. The load was applied in increments, each of which were maintained until the settlement rate was less than 0.05 mm/hour. The surface deformation was measured at four points using electronic dial gages. Each gage had a resolution of 0.0025 mm.

Figure 2.4 shows the load-settlement curves with SR1 geogrids. The depth ratio (u/B) was taken as 0.5, 0.75, and 1.0 based on previous studies that indicated the critical depth ratio ranges from 0.25 to 1.0 depending on the reinforcement layers number, spacing, and stiffness. As

observed in Figure 2.4, settlement increased as the depth of the top reinforcement layer increased. The stiffness and ultimate load carrying capacity of the plate on unreinforced soil was the smallest, while they were the greatest when the geogrid layer was placed near the surface.

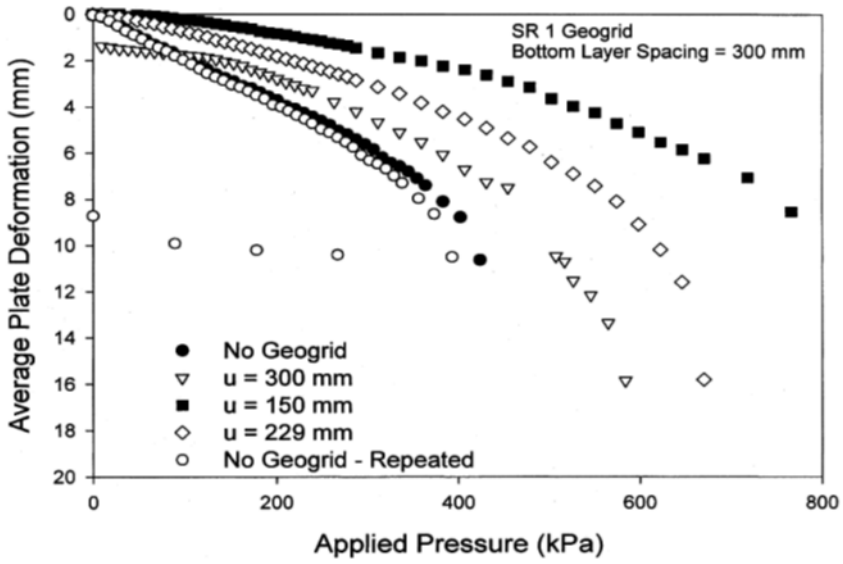

Figure 2.4 Tests performed on the sand with SR1 geogrid (Gabr and Hart 2000).

The tests which incorporated geosynthetic SR2 were performed with geosynthetic reinforcements at depths u of 150 mm, 195 mm, and 300 mm, respectively. The test with depth (u) = 150 mm was repeated with two different samples of sand. Comparing with geogrid SR1, there was improvement for the bearing capacity for the three depths, but in this case, it was consistent with the results obtained by Miyazaki and Hirokawa (1992). Gabr and Hart (2000) found that there is a critical depth ratio (u/B) in which the maximum stiffness and ultimate capacity was obtained. For depth ratios less or greater than the critical depth ratio, the bearing capacity was less than the maximum value.

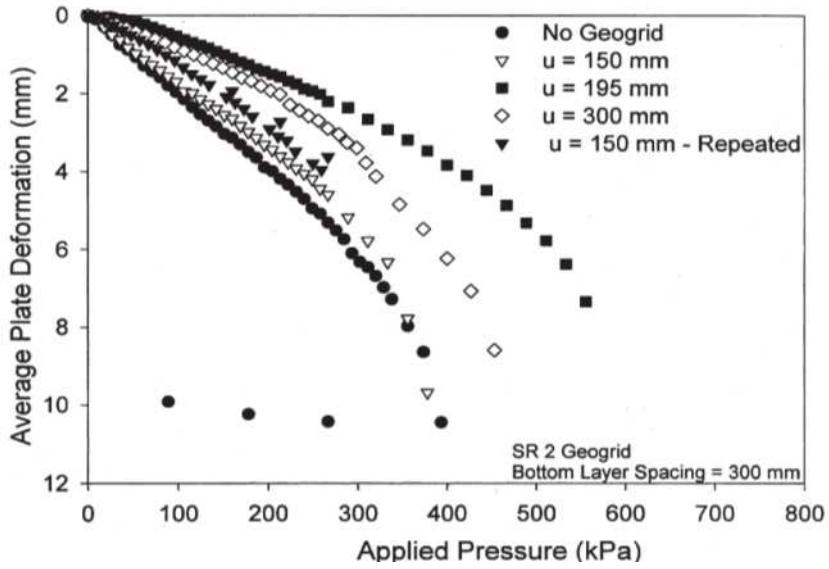

Figure 2.5 Tests performed on the sand with SR2 geogrid (Gabr and Hart, 1994).

2.3 Effect of Relative Density

The relative density of the granular fill has a significant effect on its bearing capacity because of the increase in friction angle and stiffness of the soil. Berry (1935) used 81 mm circular model footing on Ottawa sand layers having various relative densities. Figure 2.6 shows that for a constant width footing, the bearing capacity increases as the relative density (D_r) increases.

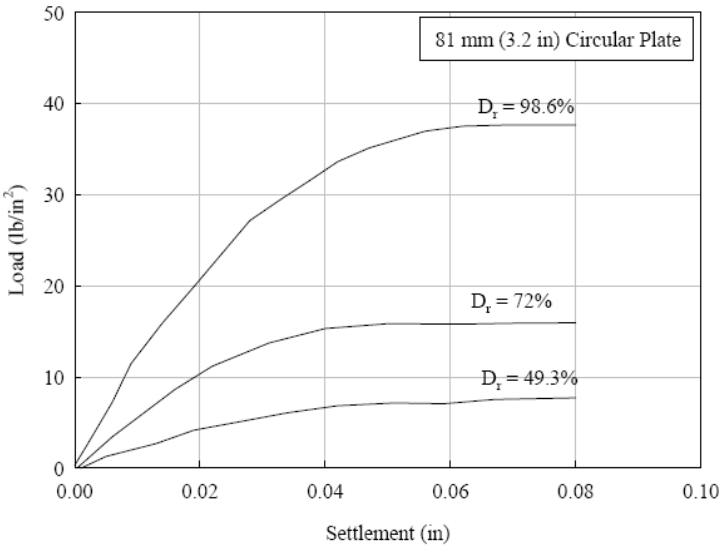

Figure 2.6 Effect of relative density on bearing Capacity (Berry 1935).

Vesic (1967) performed a comprehensive series of tests on sands with different densities using 150 mm square footing. He loaded foundations on the surface of dry uniform sand compacted to a void ratios ranging from 0.8 through 1.0. Figure 2.7 shows the influence of the sand density on the stiffness and ultimate capacity of the foundation. Further, the dense soil shows a more brittle stress-strain curve with strain softening compared to the looser soils, which is consistent with a general shear failure mode shown in Figure 2.1.

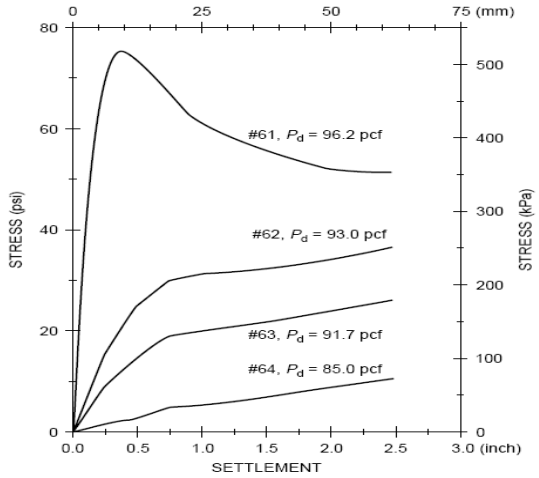

Figure 2.7 Stress versus settlement curve (Vesic 1967).

2.4 Impacts of Footing Shape

Footing shape is another important issue which can impact the load-settlement curve for foundations on reinforced soils (DeBeer 1963). There is considerable evidence that in the case of the granular materials the bearing capacity factor (N_γ) depends on the width of the footing (e.g., Hettler and Gudehus 1988; Ueno et al. 1998; Ueno 2001; Zhu et al. 2001). Berry (1935) showed that bearing capacity of circular footings on the soil surface increases with the width of a footing (0.0508, 0.0718, 0.1016, and 0.1437 m) on dense sand. This implies that the bearing capacity factor (N_γ) for the foundation will decrease as the footing size increases.

Cerato and Lutenegger (2007) evaluated the load-settlement behavior of a model-scale square and circular footing on two compacted sand layers with different characteristics. Their goal was to evaluate the impact of grain size, footing size, and relative density on the bearing capacity factor (N_y). The two different sands were tested were: Brown Mortar sand (G_s =2.69, ρ_{min}=1.41 Mg/m^3, ρ_{max} = 1.70 Mg/m^3, D_{50} = 0.6 mm, C_u = 2.1) and Winter sand (G_s=2.69, ρ_{min}=1.61 Mg/m3, ρ_{max} = 1.96 Mg/m^3, D_{50} = 1.6 mm, C_u = 4.5). These sands were compacted by hand with a 0.152 m^2 steel tamper to relative densities (D_r) of 12.6, 42.8, and 69.9% for the Brown Mortar sand and 23.7, 57.2, and 86.8% for the Winter sand. This study also evaluated the impact of footing shape, and measured the load settlement curves for square footings having widths of 25.4, 50.8, and 101.6 mm, and circular footings having diameters of 25.4, 50.8 and 101.6 mm. The model footing tests were performed in a 0.762 m × 0.762m × 0.305 m steel box with a concrete base, shown in Figure 2.8. The bearing capacity factor (N_γ) was calculated and plotted versus footing size in Figures 2.9 and 2.10. These figures show a decreasing trend in N_γ with footing width. It should be noted that these model-scale tests likely were affected by the lack of self-weight effects due to the reduced scale of the sand layer.

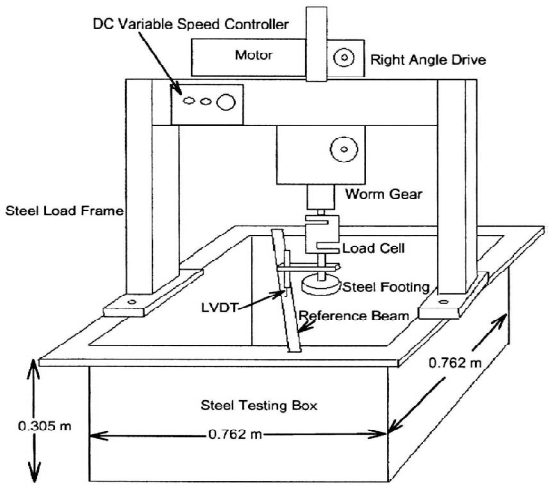

Figure 2.8 Test setup used to evaluate footing shape (Cerato and Lutenegger 2007).

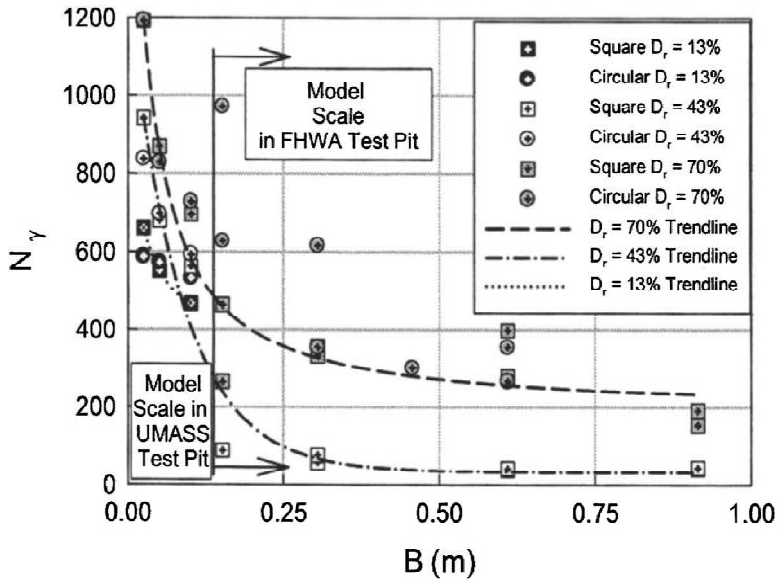

Figure 2.9 Bearing capacity factors for Brown Mortar sand (Cerato and Lutenegger 2007).

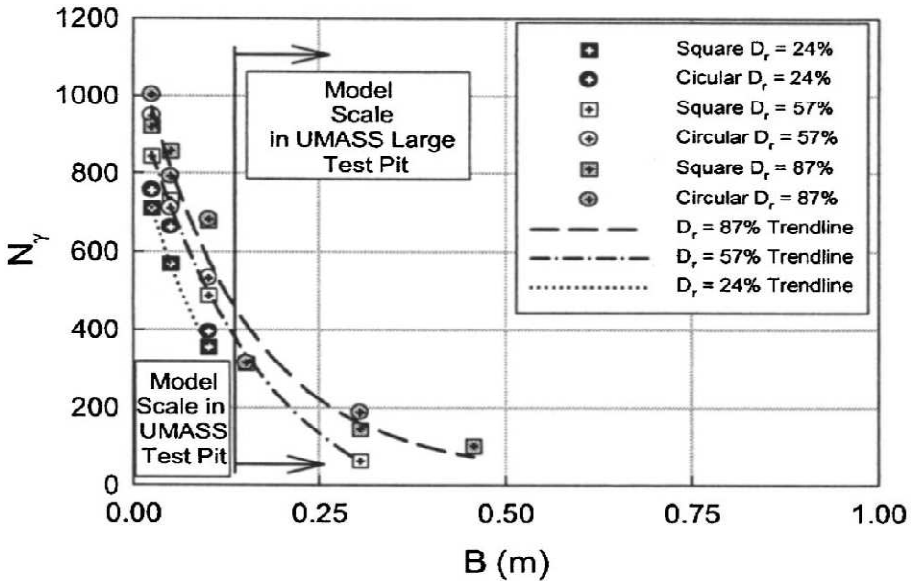

Figure 2.10 Bearing capacity factors for Winter sand (Cerato and Lutenegger 2007).

The load–settlement curves for foundations on both types of sand are presented in Figures 2.11 and 2.12. The results indicate that the relative density has a significant effect on the load settlement curve, although the footing size and shape lead to different failure modes. In general, the stiffness and ultimate bearing capacity for square footings are higher than for circular footings.

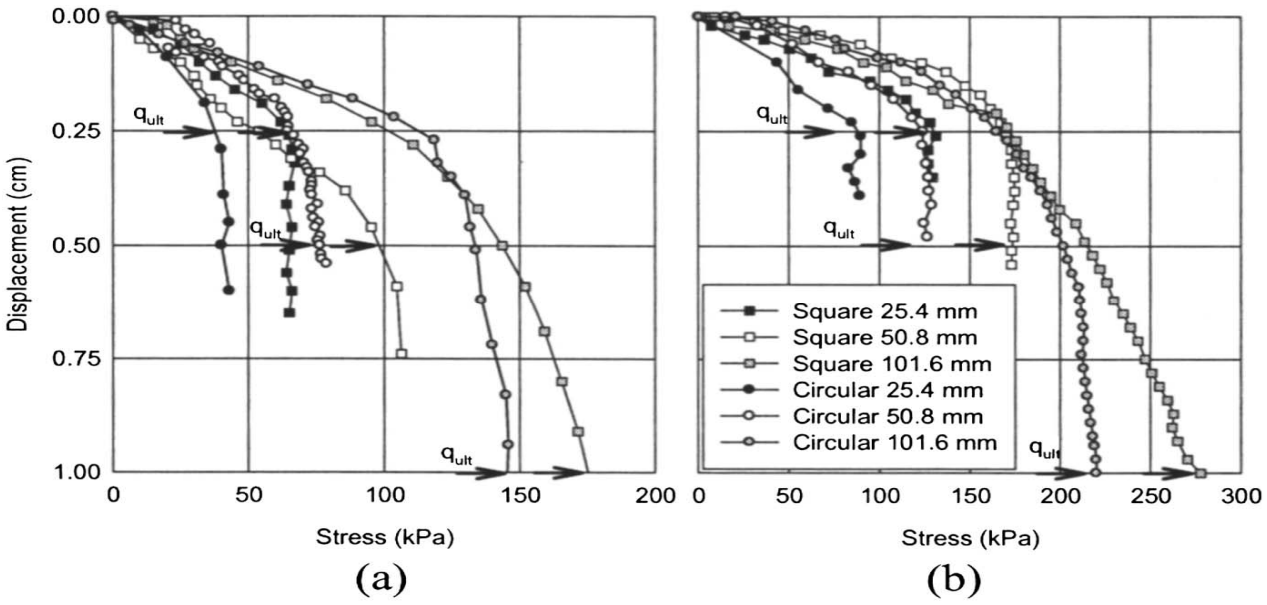

Figure 2.11 Footing load test curves for Brown Mortar sand: (a) Loose (D_r=13%; (b) Dense (D_r=70%) (Cerato and Lutenegger 2007).

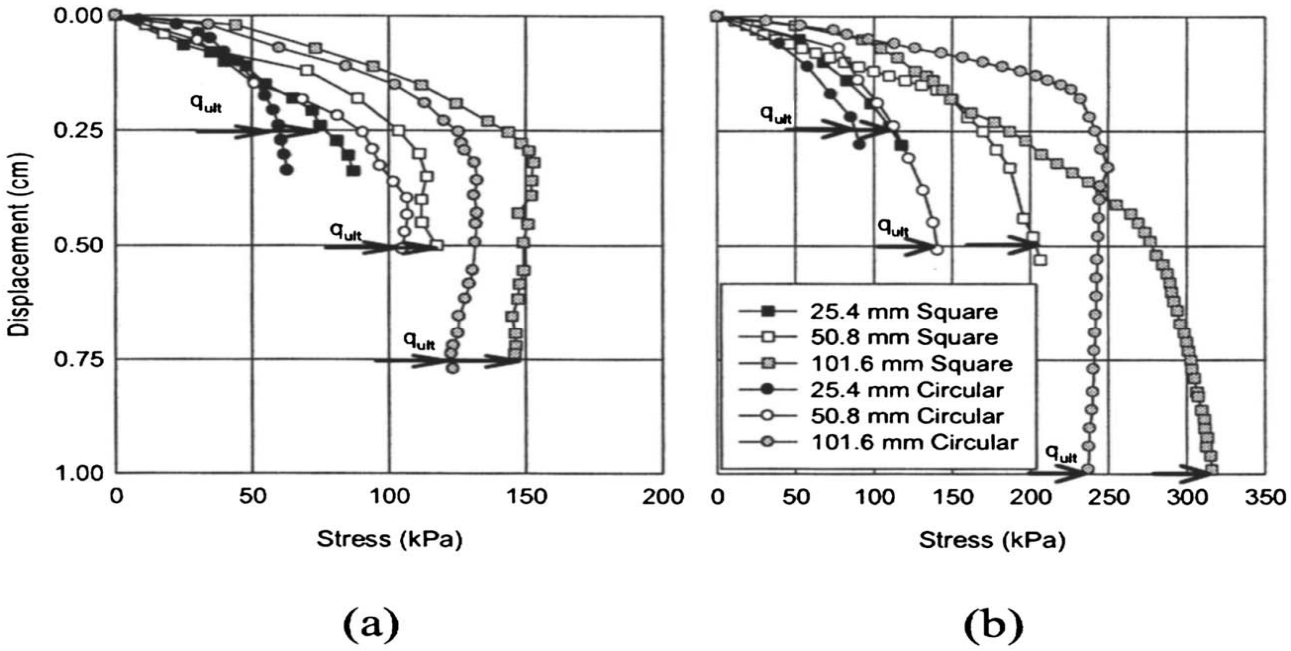

Figure 2.12 Footing load test curves for winter sand: (a) Loose (D_r=24%); (b) Dense (D_r=87%) (Cerato and Lutenegger 2007).

.

2.5 Impact of Multiple Layers of Reinforcement

The stiffness and bearing capacity increase when multiple layers of geosynthetic reinforcement are placed below the foundation (Abu-Farsakh et al., 2008; Gabr and Hart, 2000). Also, by using five layers of geogrid, they found that the settlement was reduced by 40% when they tested silty clay. Boushehrian and Hataf (2010) performed a series of tests on circular and ring footings placed on multi-layers of reinforcement layers, whose results are presented in Figure 2.13. The bearing capacity increases as the number of reinforcement layers increases, and this increase was observed up to four layers. This was also observed by Akinusuru and Akinbolade (1981).

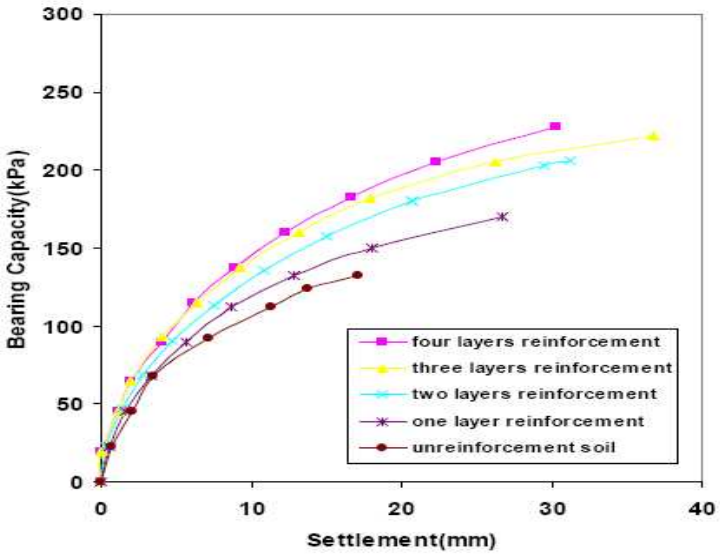

Figure 2.13 Effect of multi-layers reinforcement on bearing capacity of soil (Boushehrian and Hataf 2010).

2.6 Effect of Reinforcement Type

Dong et al. (2010) evaluated the effect of geogrid type on the bearing capacity and stiffness of reinforced granular base material. They tested three types of triangular aperture geogrids placed in a layer of Kansas River sand at a depth of 5 cm below a surface-loaded footing plate.

Their experimental test setup is shown in Figure 2.14. The Kansas River sand was placed into a box and compacted to 70% relative density. The geogrids, referred to as Geogrids I, II, and III, had triangular apertures, and differed only on the thickness of the nodes (2.1, 3.1, and 4.1 mm, respectively).

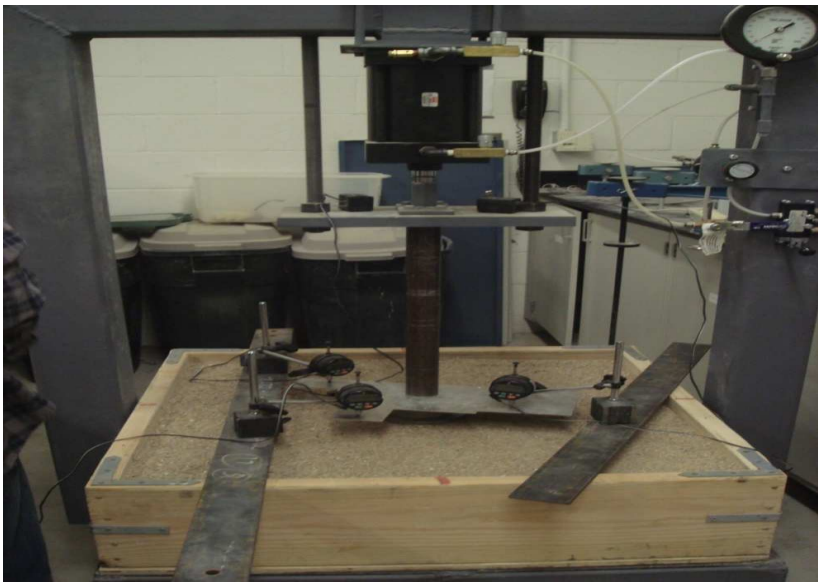

Figure 2.14 Experimental test performed by Dong et al. (2010).

The results in Figure 2.16 indicate that the geogrid type and junction characteristics may have a significant effect on the load-settlement behavior through comparison with tests on an unreinforced soil layer. Also, the results in Figure 2.15 show that the stiffness and ultimate bearing capacity of the reinforced bases increased with geogrid types I, II to III due to the greater junction strengths of each, respectively. For all tests, the geogrid-reinforced sand yielded at a displacement ranging from 5 to 10mm. All the tests on the reinforced bases showed no significant heaving which was minimized by the geogrid below the bases. As a result of that, the failure of these reinforced bases was due to the failure of sand below the geogrid.

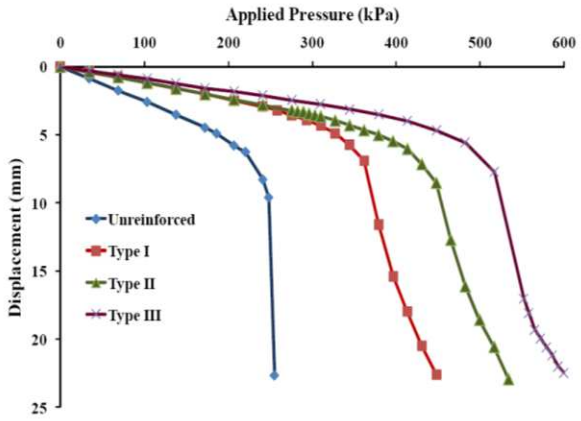

Figure 2.15 Effect of reinforcement type on the load-settlement curve (Dong et al. 2010).

2.7 Effect of Reinforcement Layer Spacing

Based on some tests to evaluate the effect of the depth of a geosynthetic reinforcement and the spacing between reinforcement layers, the bearing capacity of reinforced soil increases as the depth of the first reinforcement layer approaches the bottom surface of the footing. This is due to the high stresses that develop underneath the footing, which may cause the reinforcement to add horizontal stiffness to the granular fill. However, if the top reinforcement layer is placed at a depth less than 0.2B, where B is the footing width, the soil mass above this layer will be too thin to create enough friction to prevent the reinforcement from pulling out of the fill outside of the area of the foundation. Akinusuru and Akinbolade (1981) recommended that the first reinforcement layer should be placed at depth not more than 0.2D and the second layer at depth of 0.4D where D is the depth of the footing. Yetimoglu et al. (1994) evaluated rectangular footings on sand reinforced with planar geogrid reinforcements, and found that the highest stiffness and ultimate bearing capacity correspond to the case when the first reinforcement layer is placed at a depth of 0.25B, with a vertical spacing between two reinforcement layers of 0.2B.

Dong et al. (2010) performed tests on geogrid type II placed at depths of 5, 10, and 15cm. Their results, shown in Figure 2.16, indicate that as the depth of the geogrid layer increases, the ultimate bearing capacity and stiffness of the foundation decrease.

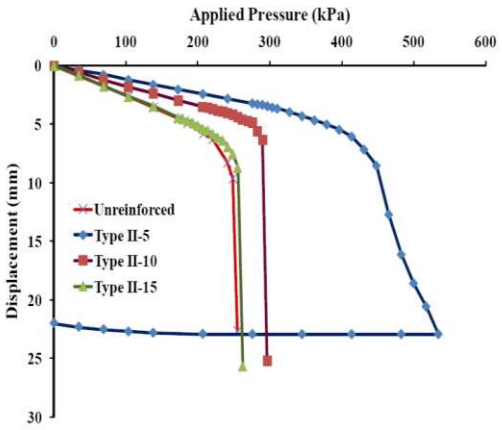

Figure 2.16 Effect of geogrid depth based on Dong et al. (2010).

2.8 Centrifuge Modeling

The main concept of the centrifuge modeling is to create a stress field in a small-size model which simulates prototype conditions in the field. Under this stress field, the results from a small-size model may be similar to those in a field-scale situation. In order to apply the same conditions as in the field, the model has to consist of the same material and have similar geometry. The model can be tested at a gravity level N in order produce complete similarity in stresses and strain as a prototype which is N times larger. Scaling relations were derived to be used to discover model measurements to represent prototype performance. According to Ko (1988), these relations can be obtained from several methods. For example, dimensional analysis using the Buckingham theorem can be used to obtain dimensionless groups of parameters that govern the phenomenon being studied. On the other hand, in situation where the phenomena being studied can be described by differential equation in terms of the field variations, it is easier to analyze theses equation to deduce the dimensionless scale factors that govern a phenomenon.

A list of scaling relations is presented in Table 2.1. These relations can be used to interpret model measurements to reflect the behavior of a prototype.

Table 2.1 Scaling Relations for Centrifuge Modeling (Ko 1988)

Quantity	Prototype	Model
Length	N	1
Velocity	1	1
Acceleration	1	N
Force	N^2	1
Stress	1	1
Strain	1	1
Energy	N^3	1
Time (Creep)	1	1
Time (Dynamic)	N	1
Time (Diffusion)	N^2	1
Frequency	1	N

The concept of modeling of models can be used to check the centrifuge model testing scheme and to validate scaling relations (Ko 1988). Also, modeling of model helps to detect when the modeling breaks down due to grain size effects, boundary effects, and strain rate effects. The concept of modeling of models is illustrated in Figure 2.17. Each of the models on the diagonal lines in this figure should have the same behavior, as long as there are no g-level dependent effects which are not considered in the scaling relations.

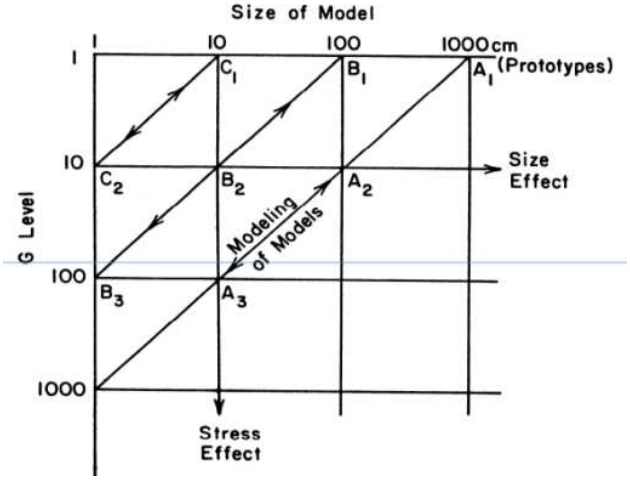

Figure 2.17 Principle of modeling of models, Ko (1988).

CHAPTER III

Experimental Setup

3.1 Centrifuge Container

The container used to define the load-settlement curves of geosynthetic reinforced soil layers was constructed from anodized aluminum with internal dimensions of 10.06 in length, 4.0 in width, and 7.0 in depth. One face of the container consisted of a 20 mm-thick Plexiglas plate to permit visual observation of deformations in the soil layer during foundation loading. A schematic of the setup is shown in Figure 3.1. A picture of the container is shown in Figure 3.2.

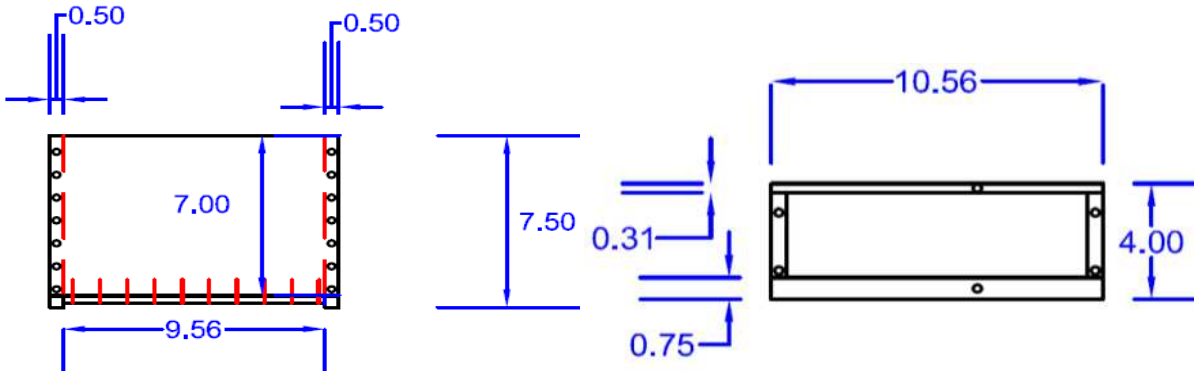

Figure 3.1 Dimensions of the container (dimensions in inches).

Figure 3.2 Centrifuge container.

3.2 Loading Apparatus

The piston used to apply loads to the foundation consists of an aluminum plate which can be attached to the side walls of the container, as shown in Figure 3.3. A hydraulic piston is mounted atop the aluminum plate. The hydraulic piston consists of an outer shell and a thin inner rod connected to a Delrin disc. When air is supplied to the outer shell, stresses are transmitted to the Delrin disc, which applies a load to the piston. The piston is connected rigidly to a load cell to measure the imposed loads.

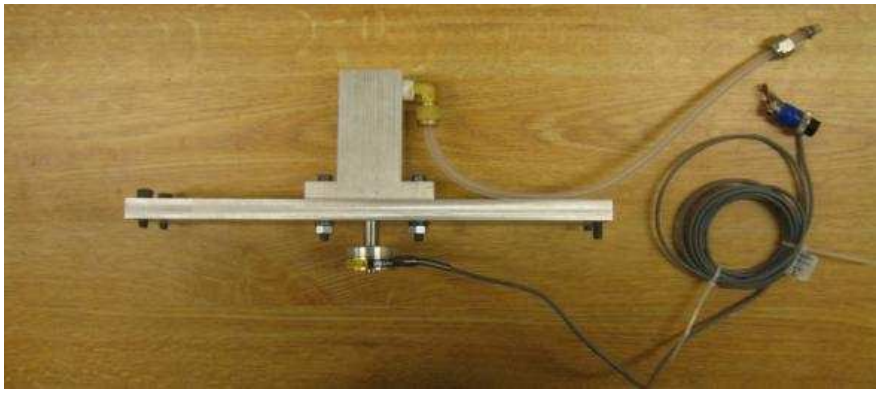

Figure 3.3 Load frame, piston, and load cell.

3.3 Footing

The primary footing used in this study is an aluminum plate with has a width of 1 inch, a thickness of 0.5 inches, and a width equal to that of the container. Accordingly, the foundation is intended to apply plane-strain loading to the soil layer. The sides of the foundation were tapered to minimize any friction with the container during loading. A dimple with a steel ball was used to permit the footing to rotate during loading. A yellow and black tape marker was attached to the side of the footing to permit digital image analysis. In the modeling of models tests, the width of the footing was increased by attaching wooden sheets to the bottom of the footing.

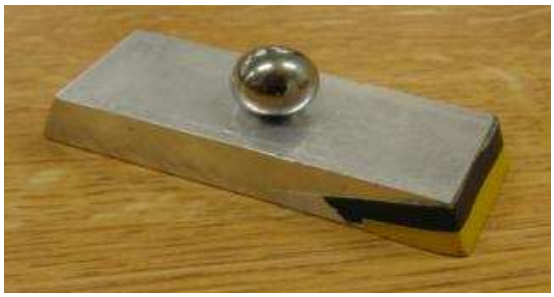

Figure 3.4 Footing with a yellow and black marker for digital image analysis.

3.4 Centrifuge

The tests in this study were performed using the instructional centrifuge at the University of Colorado at Boulder. This facility was used because the module developed in this study will eventually be used as part of an introduction to geotechnical engineering course.

Figure 3.5 Instructional centrifuge at the University of Colorado at Boulder.

The centrifuge has two baskets, one for the experimental device and the other for the counterweigh balancing. Based on that, the center of gravity must be determined in order to calculate how much weight should be placed on the counterweight arm. The center of gravity could be estimated by balancing the device on an angled ruler and measuring the distance from the base of the container to the pivot point. After the materials were placed inside the container,

the center of gravity for the whole experimental device could be calculated by determining the center of gravity of the container and the materials placed inside the container. The chart in Figure 3.6 was used to balance the centrifuge for the new centrifuge container. This chart uses the center of gravity and the weight of the container to determine how much counterweight must be placed to balance the experimental device.

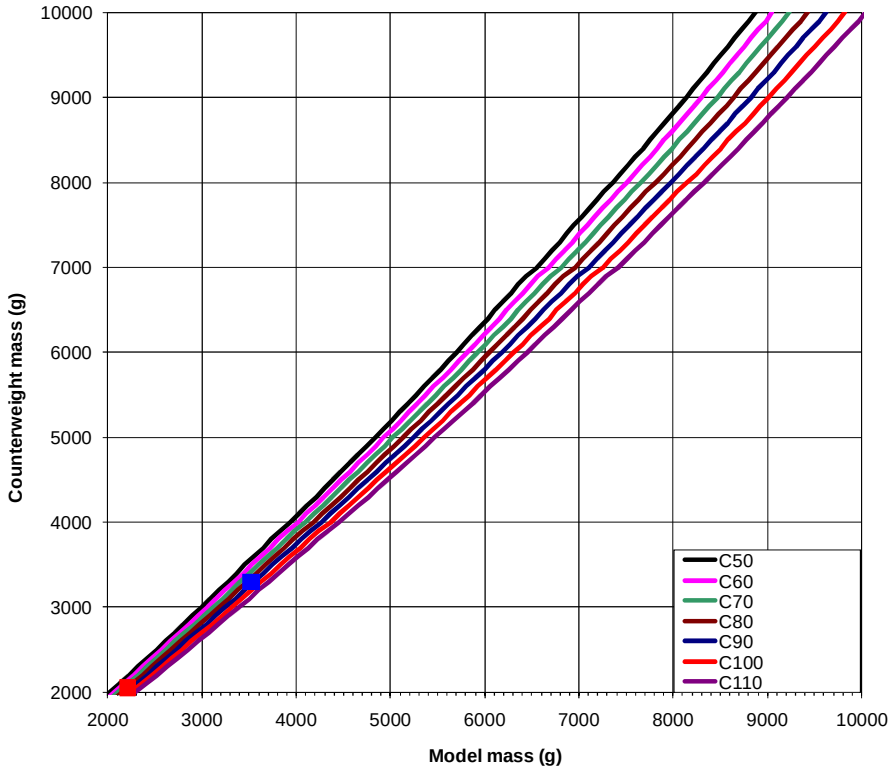

Figure 3.6 Chart for counterweight mass determination.

3.5 Instrumentation

A National Instruments data acquisition system was used to collect the data during testing, which includes the load from the load cell, the footing displacement from digital image analysis, and the gravity level from an angular velocity transducer.

A Futek 100 lb load cell was used in this study, as shown in Figure 3.7. This is a load button-type load cell with threaded mounting holes to be fixed with the piston. It has a very robust

construction available in 17-4 Stainless Steel, with a 1.25” outside diameter and a 10 feet long 26 AWG 4 conductor shielded Teflon cable.

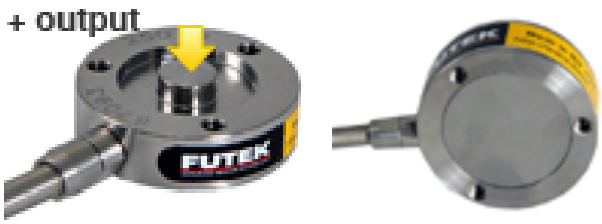

Figure 3.7 Load cell.

The load cell was attached directly to the load frame, and applies loads to a ball bearing resting in a dimple on the footing. Figure 3.8 shows the loading setup during a typical test. This design allows the footing to rotate under the applied loading.

Figure 3.8 Picture of loads being applied to the footing.

In order to monitor the displacement of the footing, a special camera was placed inside the centrifuge facing the footing. This camera is taking three pictures each almost one second. All the pictures are collected and saved in an Excel file in addition to the gravity, load, and time. The camera was designed to be able to track any record any displacement. To create a prominent edge to track, two pieces of yellow and black tape were attached to the footing.

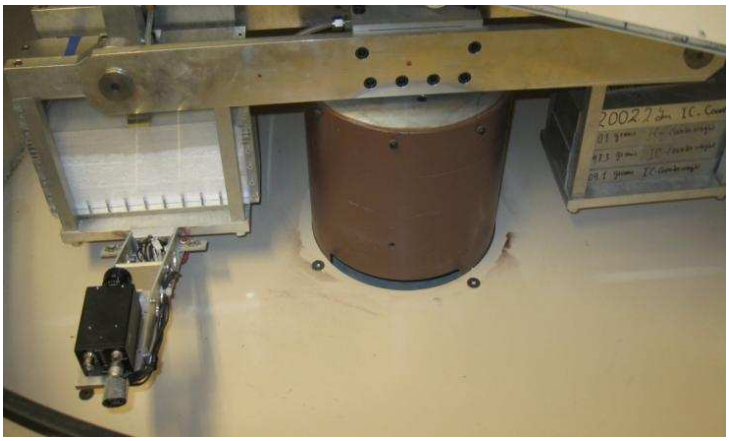

Figure 3.9 Camera used for digital image analysis.

CHAPTER IV

Materials

4.1 Geogrid

Miramesh geogrid, manufactured by Ten-Cate Mirafi Int was used in this study because it has a strength and stiffness which are approximately 10 to 20 times less than geogrids used in practice (Lee 2010). This geogrid is typically used for erosion control, an application which does not require high strength. It consists of green monofilament polypropylene yarns that are woven together to produce an open mesh grid. The Miramesh geogrid has an aperture size of 3 mm by 3 mm, a stiffness at unit strain of 206 kN/m/m, and an ultimate tensile strength 27.7 kN/m. The geogrid was cut into strips equal to the width of the centrifuge container.

Figure 4.1 Miramesh geogrid.

4.2 Granular Fill

Ottawa Sand (Grade F-75) was used as the granular fill layer in this study. It consists of Quartz grains which are 99.8% SiO_2. It has a rounded grain shape with a surface area 162 cm^2/g. The specific gravity is 2.65. A relative density test was performed to estimate the relative density value in order to control the way of preparing the sample and avoid any deference in densities

between the tests. The maximum void ratio was 0.73 and the minimum void ratio was 0.44. The maximum dry density was 1.839 gm/cm^3 and the minimum dry density was 1.53 gm/cm^3. The sand also has a coefficient of uniformity (C_u) of 1.71 and a coefficient of curvature (C_c) of 1.01. In the centrifuge modeling of the load settlement behavior of foundations on reinforced soil the grain size scale effect should be considered. Based on past studies (Yamaguchi et al. 1977), the particle size will scale up N times its original size if the soil is subjected to an acceleration of Ng. This can be evaluated using modeling of models.

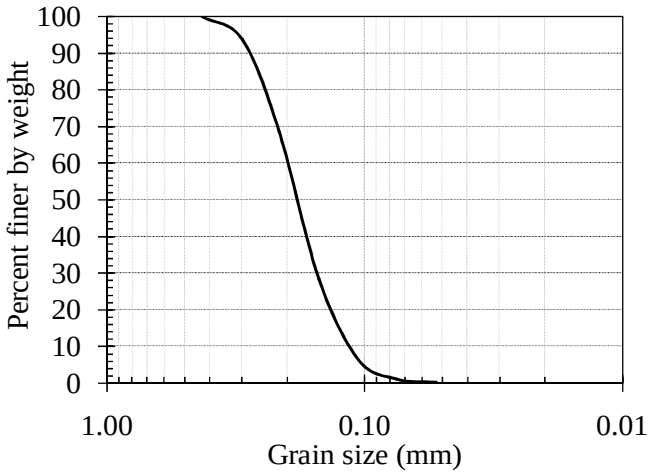

Figure 4.2 Gradation curve of the Ottawa sand.

4.3 Soft Subsurface Layer (Styrofoam)

Because the goal of this study was to evaluate the behavior of reinforced sand layers overlying a soft soil layer, it was desired to have a material which could be quickly replaced without difficult preparation procedures. Preliminary tests indicate that the bearing capacity of a thick layer of sand is high enough that addition of reinforcements would lead to a bearing capacity which exceeds the capacity of the loading system. Two different styrofoam sheets with different thicknesses were used to model layers of soft soils which were below the granular material. The maximum thickness of the soft layer is approximately 60% of the container, but

because this thickness was varied in the modeling of models tests the two styrofoam layers with different thicknesses were required. The first styrofoam sheet, which was placed directly below the sand layer, has a thickness of 1.70 cm. The other styrofoam sheet has a thickness of 7.35 cm. The thicker styrofoam sheet has a slightly greater stiffness than the thin sheet.

Figure 4.3 Styrofoam sheets (thin) used to represent the soft layers.

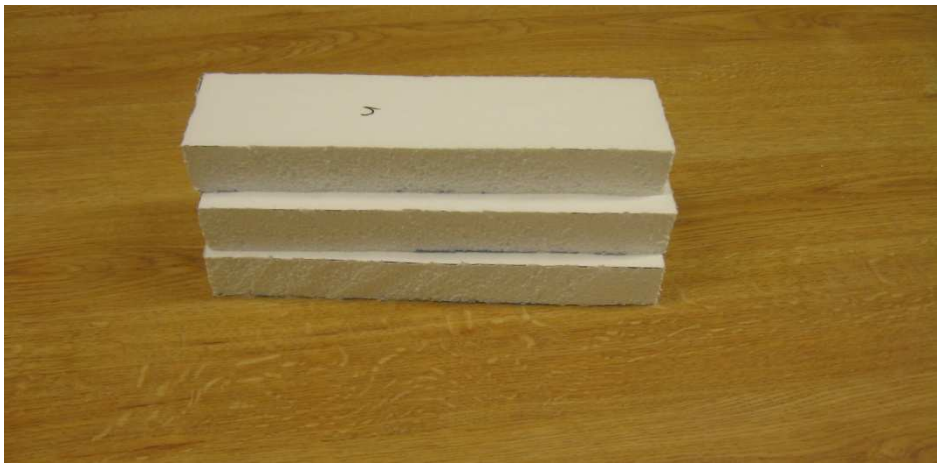

Figure 4.4 Styrofoam sheets (thick) used to represent the soft layers.

CHAPTER V

Test Procedures

5.1 Procedures

A testing program was performed in this study to evaluate the impact of incorporating geosynthetic reinforcements into a sand layer on the load-settlement behavior of the sand layer and underlying soft layer. The steps involved in performing a centrifuge bearing capacity test are summarized below:

1. The center of gravity of the centrifuge container was determined by balancing the container on an angular ruler.
2. The styrofoam sheets were stacked atop each other in the centrifuge container to represent the soft subsurface layer as shown in Figure 5.1. Because the stiffness of the two styrofoam sheets were different, they were modeled as two different layers. The initial thicknesses of the styrofoam sheets were measured, and their mass was recorded.

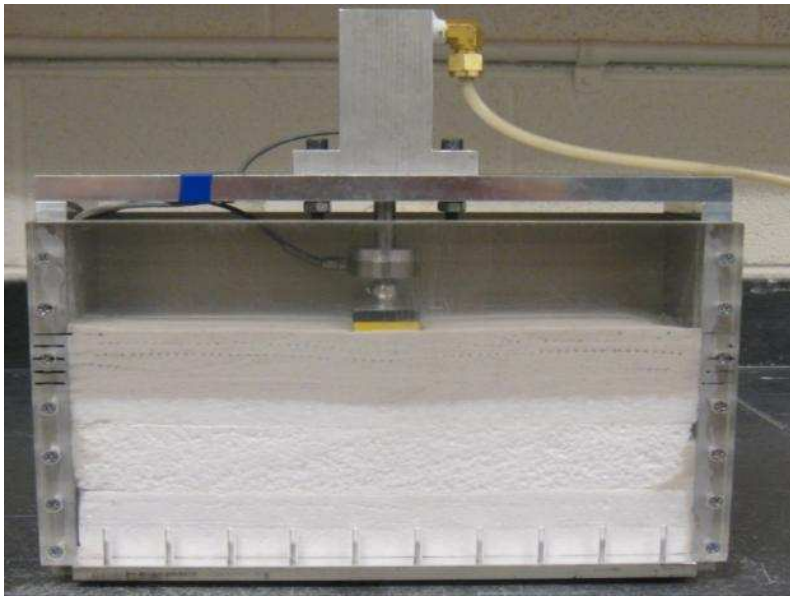

Figure 5.1 Placement of the soil layer atop the styrofoam sheets.

3. The soil was prepared by air pluviation from a constant height of 3 inches, as shown in Figure 5.2. This approach was used to control the density of the sand to minimize any differences between tests. The goal of the pluviation was to prepare a soil layer with a uniform, low relative density of approximately 40%.

Figure 5.2 Preparing the sand layer by air pluviation.

4. The geosynthetic reinforcement was placed at the desired location as shown in Figure 5.3 and sand pluviation was continued beyond this level.

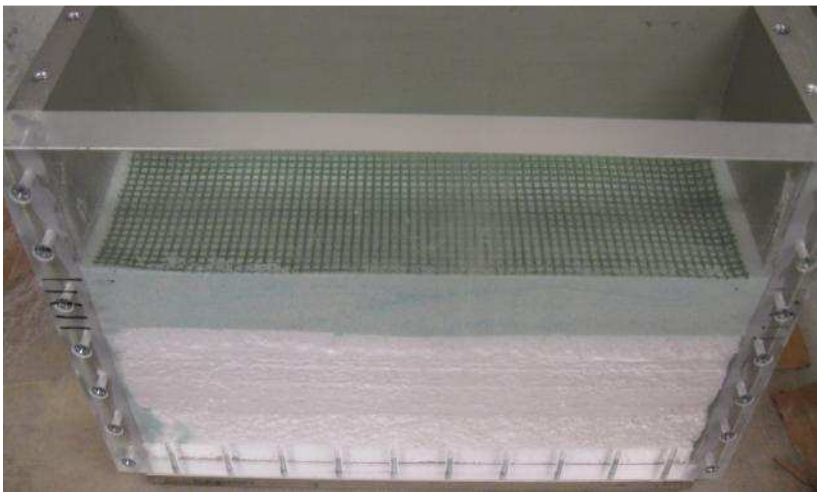

Figure 5.3 Placement of the geogrid layer.

5. After preparation of the soil layer, the load frame was attached to the centrifuge container, and the experimental device was weighted. The relative density was calculated using the known volume and mass of the soil layers.
6. The center of gravity was calculated for the device including the soil based on the heights and masses of the different layers (and the mass and center of gravity of the container). Based on the chart presented in Figure 3.6, the required counterweight was determined.
7. The experimental setup was placed in the centrifuge, and the instrumentation cable for the load cell was connected to the data acquisition system. The air pressure tube for the loading piston was also connected to the fitting on the slip-ring stack.
8. The lid of centrifuge was closed and a target centrifuge acceleration level was imposed by the centrifuge.
9. After the target gravity level was reached, the load was applied to the footing by manually adjusting the pressure using an air regulator. The load was applied in 1 psi increments until the displacement recorded using the digital image analysis reached a stable value. The measured load, footing settlement, and g-level was recorded into an Excel file using the LabView data acquisition system.

Figure 5.4 Control panel for the loading system (air pressure regulator).

5.2 Testing Matrix

Four testing series were performed as part of this study. These include:

1. Evaluation of the load-settlement behavior of styrofoam under different centrifuge acceleration levels.
2. Evaluation of the load-settlement behavior of unreinforced sand under different centrifuge acceleration levels.
3. Evaluation of the impact of centrifuge acceleration level on the plane-strain plate-load stiffness of soil layers having geosynthetics placed at different depths from the soil surface. In these tests, the same geometry was used in all of the soil layers, so the tests were not performed centrifuge modeling principles. The goal of this test series was to evaluate the impact of confining pressure on the pullout behavior of the geosynthetic reinforcement when placed at different depths. In different tests, a geogrid was placed at depths 0.25B, 0.5B, 0.75B, and 1.0B. An additional test was evaluated for multiple geogrids in the soil layer.
4. Evaluation of the capacity of foundations on reinforced soil involving modeling of models following conventional centrifuge modeling principles.

CHAPTER VI

Results

6.1 Styrofoam Test Series

A styrofoam system was assembled in the container without the presence of the soil layer to evaluate the stiffness of the styrofoam sublayers. A schematic of the styrofoam system incorporating both styrofoam types is shown in Figure 6.1.

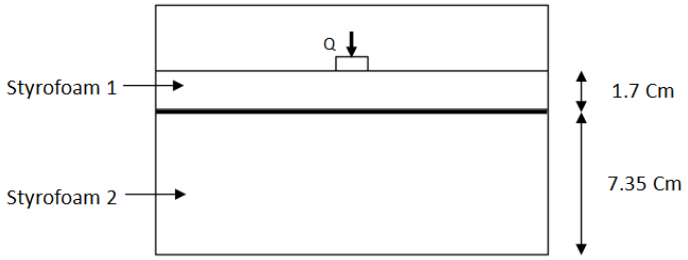

Figure 6.1 Schematic of the styrofoam system incorporating both styrofoam sheets.

The results shown in Figure 6.2 indicate that there is no dependence of self weight on the stiffness of the styrofoam system. This is also consistent with the load-settlement curves of the styrofoam when the load is plotted on a logarithmic scale, as shown in Figure 6.3.

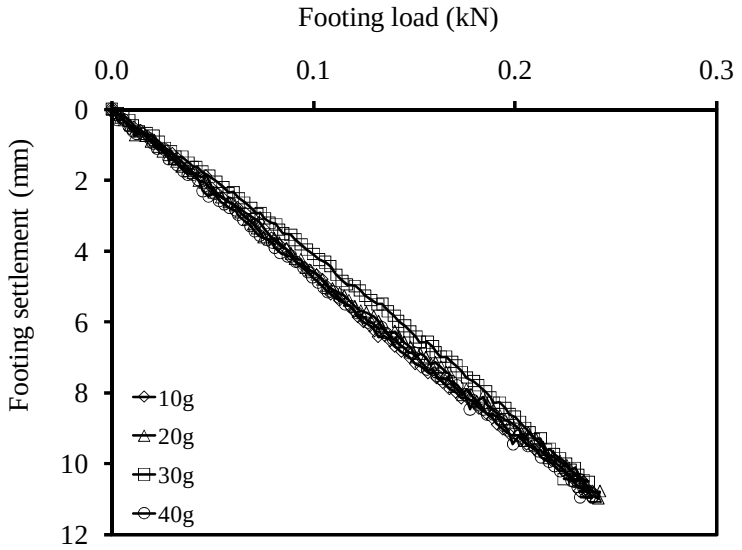

Figure 6.2 Load-settlement plot for the styrofoam system (model scale, natural scale).

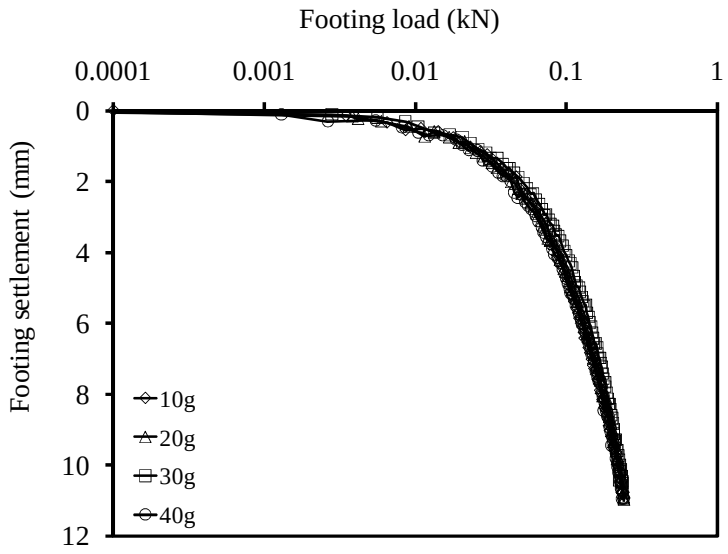

Figure 6.3 Load-settlement plot for the styrofoam system (model scale, logarithmic scale).

6.2 Tests on Unreinforced Soil under Different Gravity Levels

Unreinforced soil was tested at different gravity levels with the same footing width to evaluate the effect of the gravity and particle self-weight on the stiffness of the foundation load-settlement curve. The dry and relative soil densities are presented in Table 6.1 for each test..

Table 6.1. Dry densities and relative densities for unreinforced soil tests.

G-Level	Soil density (gm/cm^3)	Relative density (%)
10	1.634	37.93
20	1.632	37.40
30	1.632	37.42
40	1.633	37.61

The load settlement curves for the series of tests on unreinforced soil layers are shown in Figure 6.4, in model scale. In these tests, the load required to displace the footing by 2.5 to 6.5 mm was recorded. Under low gravity levels, it was not possible to reach higher displacements than 6.5 mm due to rotation of the footing. The results in Figure 6.4 indicate that the g-level leads to a stiffening of the soil layer at low levels of displacement, but at high displacements, the

g-level did not have a significant impact. It should be noted that the tests in this section all have the same footing geometry, so they are not models of models. However, they emphasize the importance of soil self-weight on the resistance to footing loading.

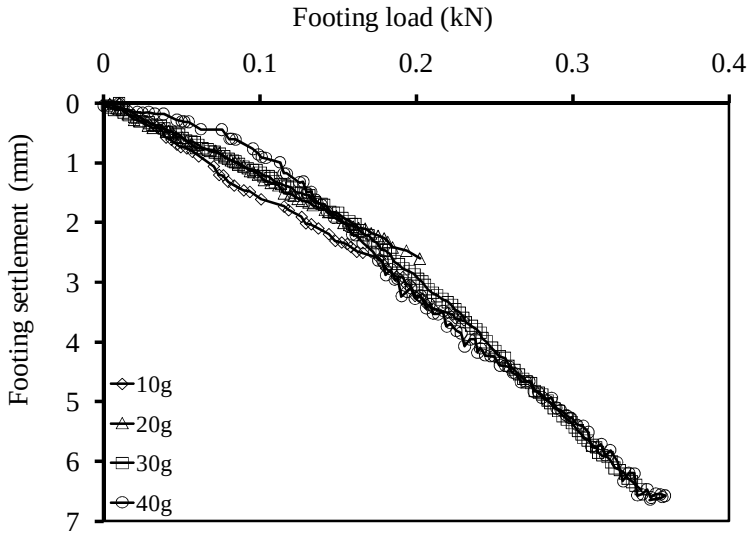

Figure 6.4 Load-settlement curves of soil layers (Model scale, natural scale).

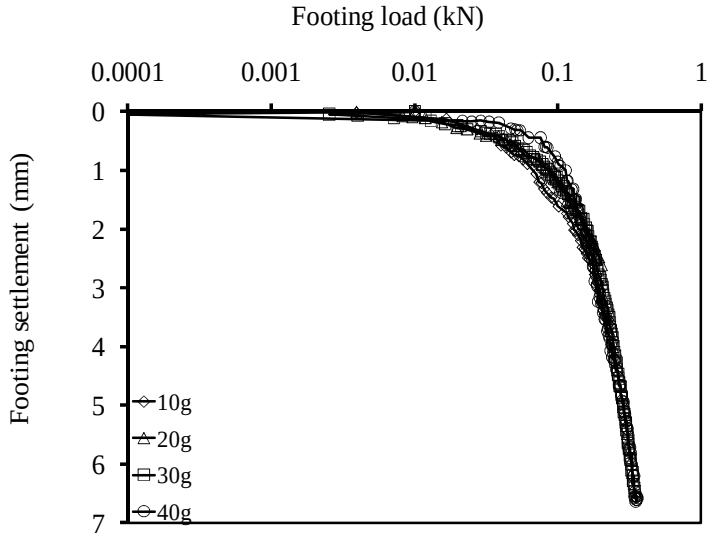

Figure 6.5 Load-settlement curves of soil layers (Model scale, logarithmic scale).

6.3 Tests on geosynthetic reinforced soils

A series of tests were performed on geosynthetic-reinforced soil layers under different gravity levels to evaluate the impact of soil self-weight on the load-settlement curve. As a baseline case, a soil layer having a thickness of 1.5B (where B is the width of the footing) was placed atop the styrofoam layers without reinforcement. Further, geosynthetics reinforcements were placed at different depths from the foundation ranging from 0.25B to 1B (listed as fractions of the footing width B) in a soil layer having a thickness of 1.5B. Further, one scenario was evaluated in which several geosynthetic reinforcements were included at different depths. Similar to the soil-only tests, the Ottawa sand layer was prepared using air pluviation, and the dry and relative densities are presented in Table 6.2.

Table 6.2. Dry densities and relative densities for all tests.

Test	Dry density (gm/cm^3)			Relative density (%)		
	1G	20G	40G	1G	20G	40G
No geogrid	1.628	1.628	1.631	35.99	36.05	36.96
Geogrid at depth 0.25B	1.635	1.633	1.633	38.50	37.62	37.85
Geogrid at depth 0. 5B	1.634	1.631	1.630	38.03	37.14	36.63
Geogrid at depth 0.75B	1.632	1.698	1.631	37.46	37.56	37.13
Geogrid at depth 1B	1.635	1.631	1.629	38.44	36.93	36.47
Geogrid at depths 0.25B, 0.5B, and 0.75B	1.638	1.629	1.631	39.47	36.25	37.09

The load settlement curves for the series of tests on unreinforced and reinforced soil layers under 1G (no centrifugation) are shown in Figure 6.6. In these tests, the load required to displace the footing by 2 to 3 mm was recorded. In these tests, higher displacements similar to the soil-only tests were not possible because of rotation of the footing under 1G conditions. This likely occurs because of instabilities caused by the low self-weight. The load settlement curves show a hardening behavior which is different from the unreinforced soil, which can be attributed to the mobilization of the geogrid tension at higher displacement levels. The geogrid did not lead to a change in the initial stiffness of the soil layer.

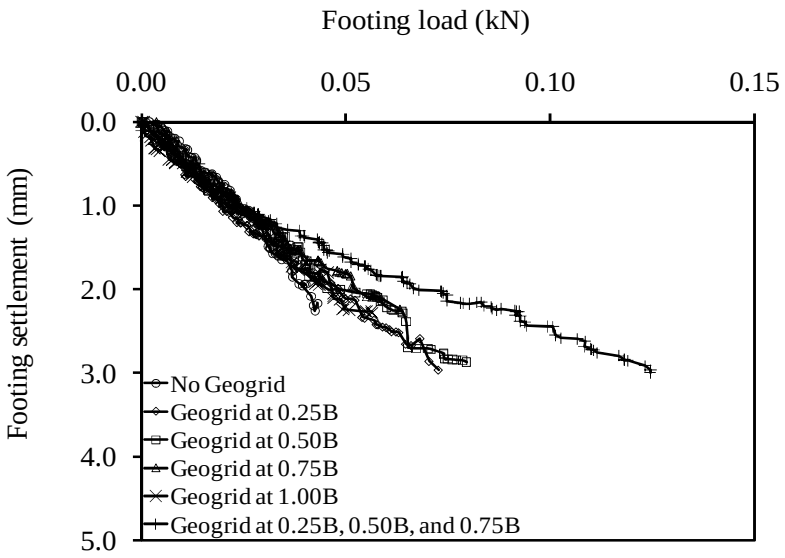

Figure 6.6 Load-settlement plot for tests under 1G (Model scale, natural scale).

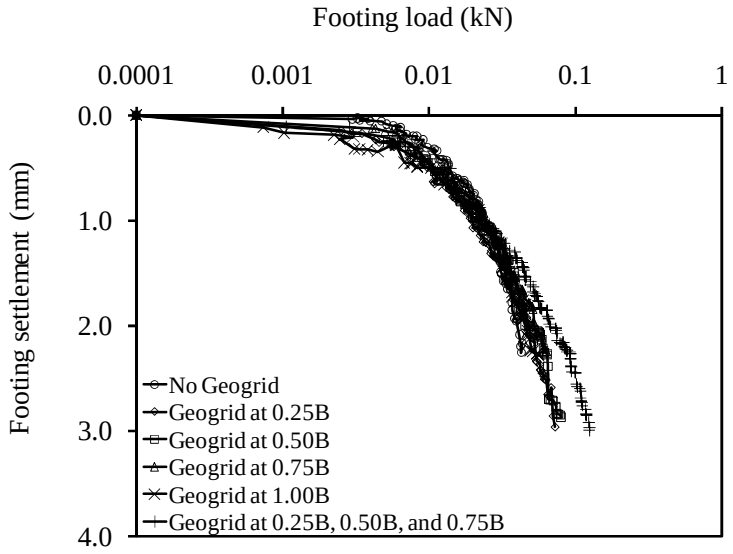

Figure 6.7 Load-settlement plot for tests under 1G (Model scale, logarithmic scale).

The load settlement curves for the series of tests on unreinforced and reinforced soil layers under 20G are shown in Figure 6.8. In all of these figures, it can be seen that the reinforced and unreinforced soil are behaving at the same way at the beginning of loading where the geogrid started bending and pulling down causing the same displacement as in unreinforced soil. By the end of the loading where the load is higher, the geogrid will start showing resistance, by friction

and soil stiffness under the geogrid, to pending and pulling down. Therefore, penetrating of the geogrid to the soil will be reduced and the settlement in reinforced soil will be less comparing with the unreinforced soil.

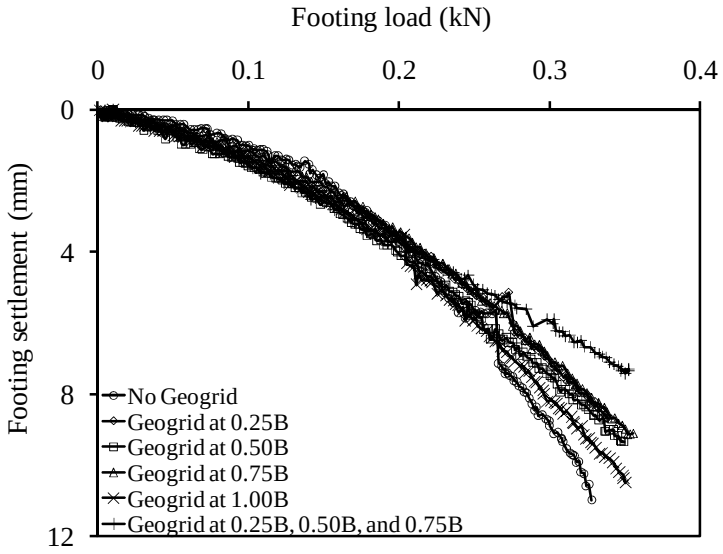

Figure 6.8 Load-settlement plot for tests under 20G (Model scale, natural scale).

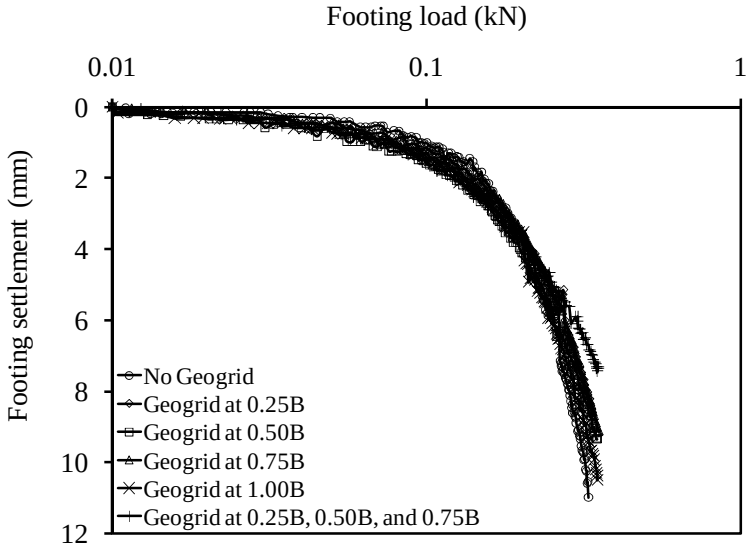

Figure 6.9 Load-settlement plot for tests under 20G (Model scale, logarithmic scale).

The load settlement curves for the series of tests on unreinforced and reinforced soil layers under 40G are shown in Figure 6.10. Similar results to the previous cases are observed, in which

the reinforced and unreinforced soil layers showing similar load-settlement curves at the beginning of loading. At the end of the loading, the geogrids start mobilizing tension and contribute to the load-settlement behavior of the reinforced soil.

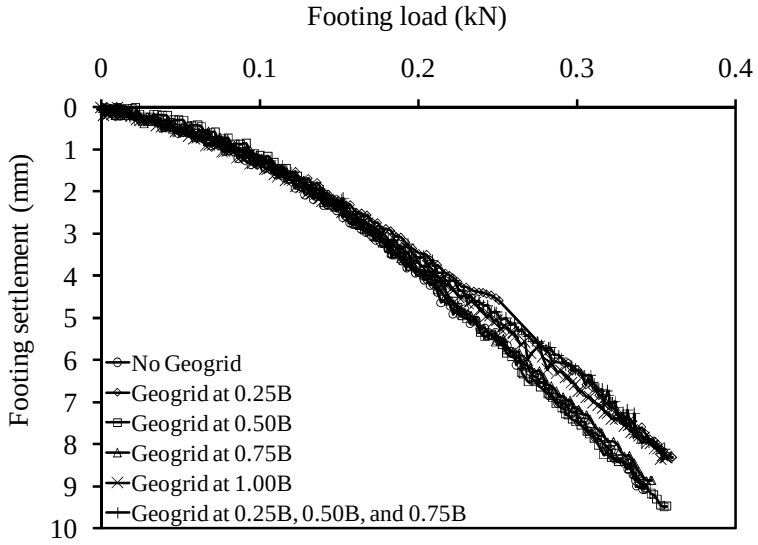

Figure 6.10 Load-settlement plot for tests under 40G (Model scale, natural scale).

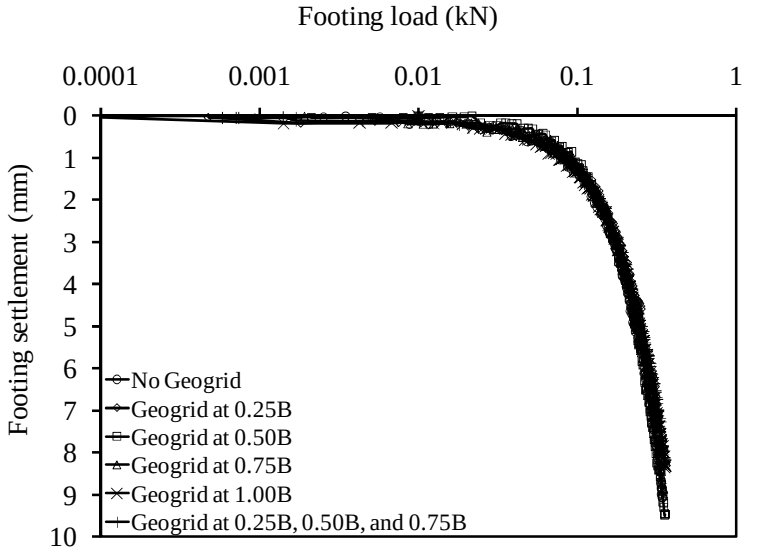

Figure 6.11 Load-settlement plot for tests under 40G (Model scale, logarithmic scale).

6.4 Modeling of Models

Three models were evaluated in this study at gravity levels of 20G, 30G, and 40G. The footings used in each of these tests had widths of 1.5 inches, 2.0 inches, and 4.0 inches, respectively. The same container was used in three modeling tests, but the thickness of the soil layers was varied so that the stress distribution was equal in each tests. The details of the modeling of models tests are presented in Table 6.3, and the results of the tests are shown in Table 6.4 in prototype scale.

Table 6.3 Details of the modeling of models tests.

Description	G-level	Model				Prototype			
		Sand Layer Thickness (mm)	Soft Layer Thickness (mm)	Footing Width B (mm)	Geogrid Depth (mm)	Soil Layer Thickness (mm)	Soft Layer Thickness (mm)	Footing Width B (mm)	Geogrid Depth (mm)
No geogrid	20	34	34	51	0	680	680	1016	0
No geogrid	30	23	23	34	0	680	680	1016	0
No geogrid	40	17	17	25	0	680	680	1016	0
Geogrid at 0.25B	20	34	34	51	13	680	680	1016	254
Geogrid at 0.25B	30	23	23	34	8	680	680	1016	254
Geogrid at 0.25B	40	17	17	25	6	680	680	1016	254

Table 6.4 Results from the tests in prototype scale.

Description	G-level	Prototype		
		Applied load (kN)	Settlement measured (mm)	Secant stiffness (kN/mm)
No geogrid	20	115	40.73	2.544
No geogrid	30	146	50.51	6.815
No geogrid	40	213	59.39	7.436
Geogrid at 0.25B	20	115	40.77	2.520
Geogrid at 0.25B	30	146	48.01	6.864
Geogrid at 0.25B	40	213	56.97	7.485

The load settlement curves for the three models are shown in model scale in Figure 6.12 and in prototype scale in Figure 6.13. This figure indicates that the tests at a higher g-level had a softer response with a smaller capacity. No significant difference was noted between the reinforced and unreinforced soil layers at each of the g-levels. The results shown in prototype scale have similar load settlement curves, indicating that the boundary conditions, grain size, or strain conditions are similar between each of the models.

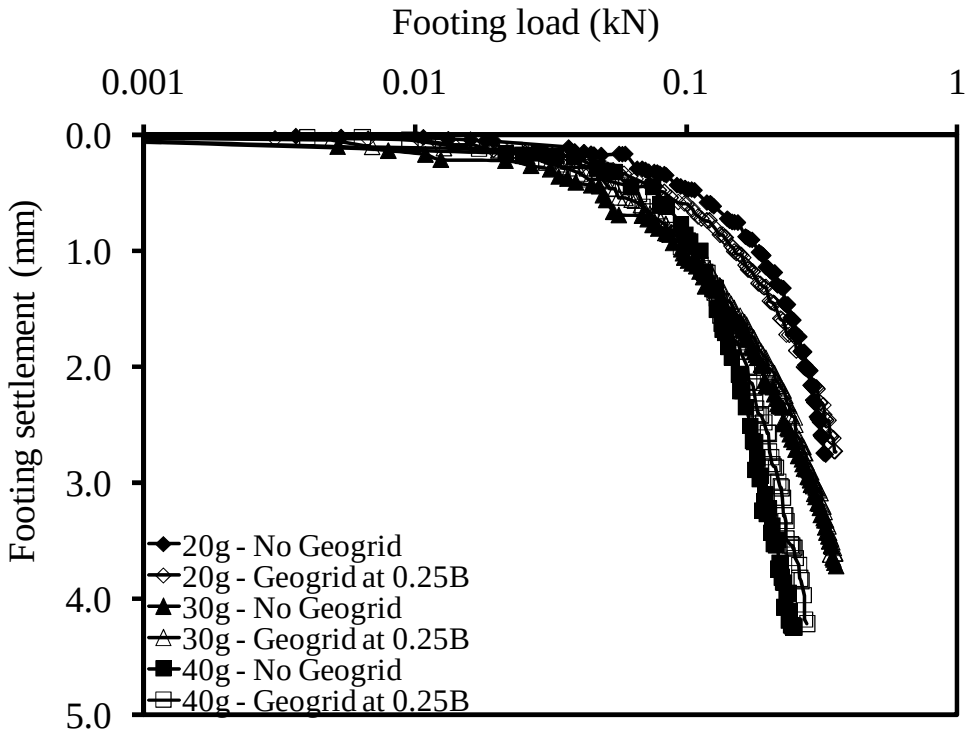

Figure 6.12 Modeling of models for load settlement curves of reinforced soil layers (Model scale, logarithmic scale).

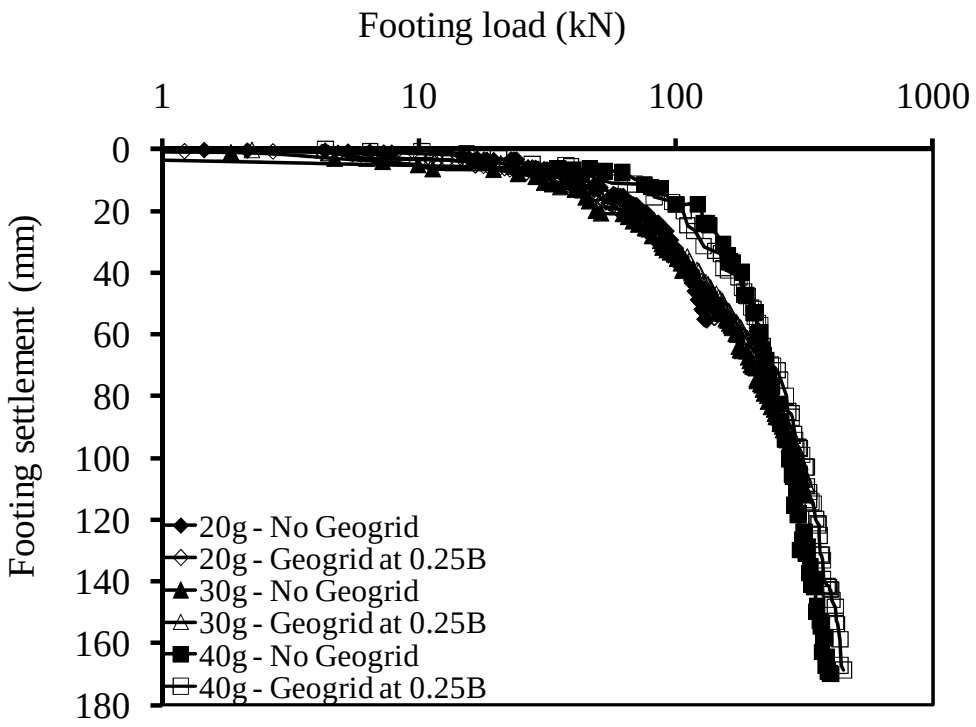

Figure 6.13 Modeling of models for load settlement curves of reinforced soil layers (prototype scale, logarithmic scale).

CHAPTER VII

Analysis

7.1 Secant stiffness

The secant stiffness was calculated from the measured load-settlement curves by assuming that the load-settlement curve is hyperbolic (Chin and Vail, 1973), as follows:

(7.1) $$Q_{fit} = \frac{S}{AS+B}$$

where S is the vertical footing settlement and Q_{fit} is the fitted load. The constants A and B can be evaluated by rearranging the above equation to the below equation and plotting S/Q versus S. The best fit straight line will give an intercept of B and a slope of A. When interpreting these constants, 1/B is the initial stiffness of the hyperbola, while 1/A is the ultimate value of the hyperbola. This method was found to be unsuitable for definition of the capacity of the foundation, because the hyperbolic model tended to significantly overestimate the maximum load applied in the test (Duncan et al. 1970). Nonetheless, the fitted relationship for Q as a function of S was useful in calculation of the secant stiffness at any value of settlement.

(7.2) $$\frac{S}{Qfit} = AS + B$$

A typical fit of S/Q - S is shown in Figure 7.1. The data was fit so that the fitted hyperbola matched the initial stiffness of the curve, not the ultimate capacity.

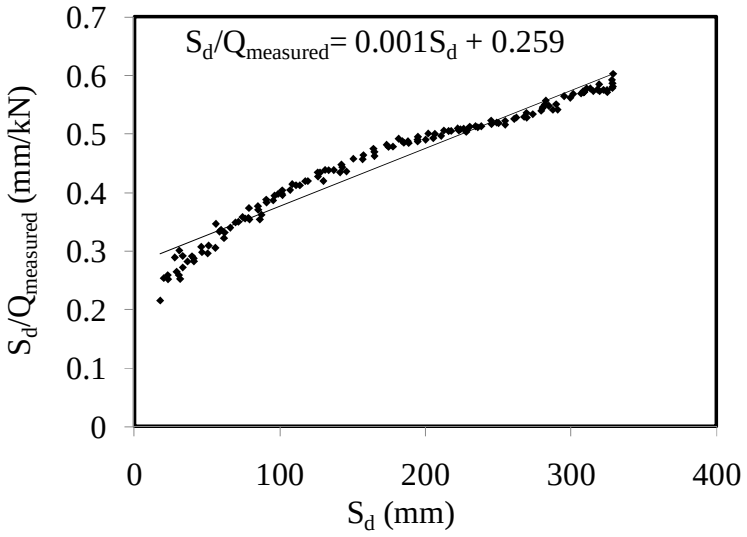

Figure 7.1 Modified Q-S curve for Kondner fitting of a hyperbola.

After the values of A and B were determined using the above approach, the secant stiffness corresponding to any settlement can be calculated as follows:

(7.3) $M = Q_{fit}/S_d$

where M is the secant stiffness (units of kN/mm) at a characteristic settlement S_d. In this study, all of the values of secant stiffness were corresponding to the settlement of S_d = 0.5B. Calculating the secant stiffness with incorporated settlement will show the differences between the reinforced and unreinforced soil, depth and number of the geogrid effect, and the gravity effect. The following tables and figures summarize the secant stiffness corresponding to the settlement of 0.5B for soil only, styrofoam only, and reinforced soil at different gravity levels.

Table 7.1 Stiffness defined as the load corresponding to a settlement of 0.5B in Model Scale – Styrofoam only.

g-level	M (kN/mm)
10	0.022
20	0.022
30	0.022
40	0.022

Table 7.2 Stiffness defined as the load corresponding to a settlement of 0.5B in Model Scale – Soil only.

g-level	M (kN/mm)
10	0.051
20	0.053
30	0.053
40	0.054

Table 7.3 Stiffness defined as the load corresponding to a settlement of 0.5B in Model Scale – Reinforced soil

Geogrid Depth (XB)	1g M (kN/mm)	20g M (kN/mm)	40g M (kN/mm)
0	0.0093	0.0268	0.0288
0.25	0.0105	0.0271	0.0289
0.5	0.0106	0.0272	0.0289
0.75	0.0106	0.0269	0.0289
1	0.0104	0.0269	0.0288
Multiple	0.0109	0.0275	0.0288

From Figure 7.2 presented below, there is no effect of gravity on the stiffness of the styrofoam sheets. All of the secant stiffness values correspond to the same displacement of 0.5B.

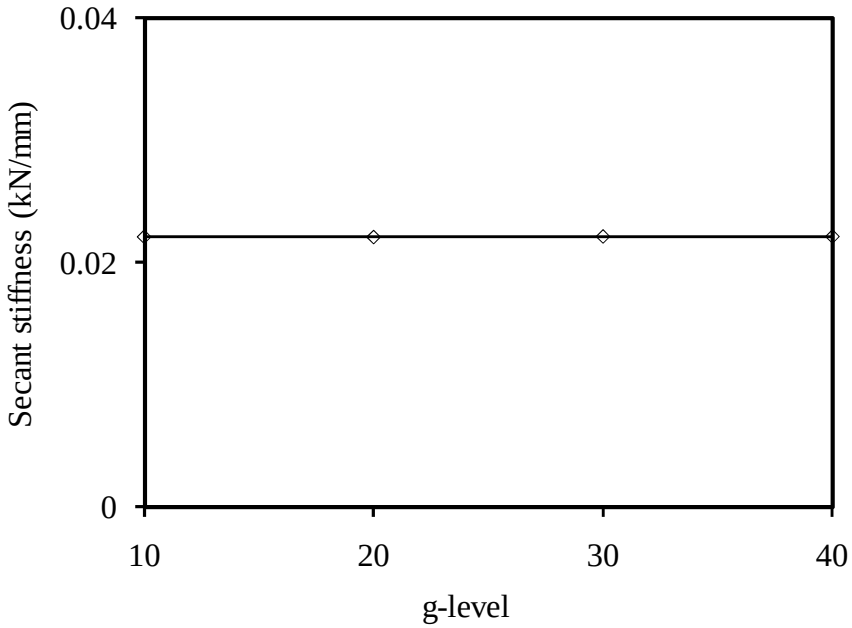

Figure 7.2 Secant stiffness of styrofoam under different gravity levels.

The secant stiffness of the unreinforced soil layer is shown in Figure 7.3 as a function of the gravity level. Although a slight increasing trend is noted, the stiffness of the soil layers is approximately constant with gravity level.

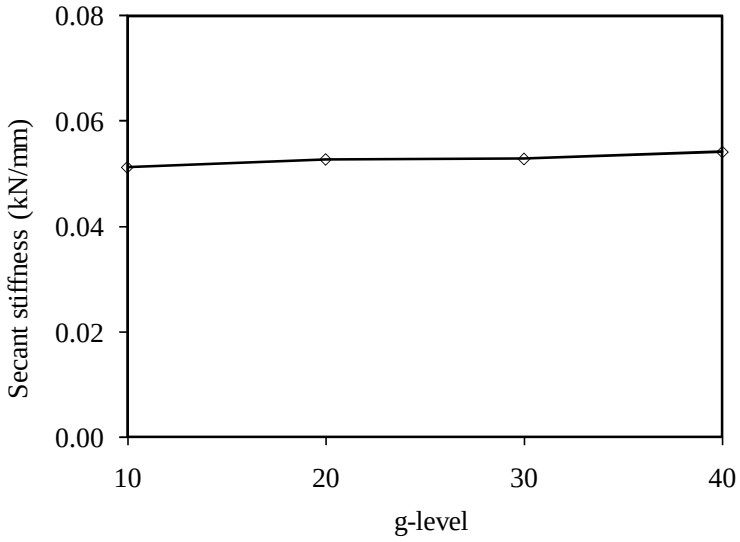

Figure 7.3 Secant stiffness of soil under different gravity levels.

In Figure 7.4, a summary chart for the tests under different gravity level is presented, this figure emphasizes that the soil self-weight has little impact on the load-settlement behavior of footings on geosynthetic reinforced granular fills overlying soft soil.

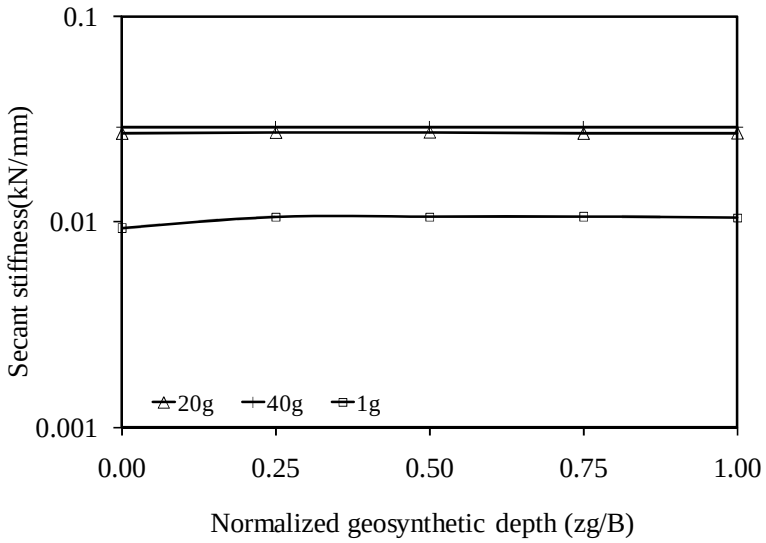

Figure 7.4 Secant stiffness of reinforced soil layers under different g-levels.

7.2 Settlement Model

To evaluate the effect of the geosynthetic that was used in this research, several linear elastic theories to determine the settlement will be used. These theories used by Vakili (2008) to determine the settlement of a layered system loaded using a rigid plate having a diameter *a* and a footing stress *q*, given the elastic parameters of the individual layers. Vakili (2008) combined the analysis of Thenn de Barros (1966) with that of Palmer and Barber (1940). Thenn de Barros (1966) showed how the upper two layers in a three layer system could be replaced by a single layer having an equivalent modulus E_e. According to that regards, the two top layers in our system will be having an equivalent modulus of:

(7.4) $$E_e = \left(\frac{h_s \sqrt[3]{E_s} + h_1 \sqrt[3]{E_1}}{h_s + h_1}\right)^3$$

where h_s and h_1 are the thickness of the granular material and the thin layer of the styrofoam, respectively, E_s and E_1 are the Young's modulus of the granular material and the thin Styrofoam layer, respectively. Palmer and Barber (1940) showed that the two top layers can be replaced by a single layer having Young's modulus of E_2 and Poisson's ratio of v_2, but with a thickness of:

(7.5) $$he = (h_S + h_1)\left(\frac{E_e(1-v_2)^2}{E_2(1-v_2)^2}\right)^{1/3}$$

The Young's modulus for the granular fill and the styrofoam sheets were determined by performing one load-settlement test for each layer and using the following approach for calculating the Young's modulus (Schleicher 1926):

(7.6) $$S_d = C_d\, q\, B\left(\frac{1-v^2}{E}\right)$$

where the following variables can be defined as S_d is the vertical settlement of any point on the surface of an elastic half-space subjected to a footing load q, B is the width of the footing, v is the Poisson's ratio of a layer, E is the Young's modulus of a layer, and C_d is a parameter which accounts for the shape of the loaded area and position of the point for which the settlement is being calculated. Equation 7.2 can be written in terms of M, as follows:

(7.7) $$E = \frac{C_d M}{B}(1-\nu^2)$$

Based on the model of Vakili (2008), the vertical settlement of a footing on a layered system of elastic materials can be calculated as follows:

(7.8) $$W_z = \left(\frac{2(1-v_2{}^3)qa}{E_2}\right) + \left\{k^3 + (1-k^3)\left[\sqrt{1+\left(\frac{m}{k}\right)^2} - \left(\frac{m}{k}\right)\right] x \left[1 + \frac{m}{2k(1-v_2{}^3)}\sqrt{1+\left(\frac{m}{k}\right)^2}\right]\right\}$$

where the parameters m and k are parameter are defined as follows:

(7.9) $$m = \frac{h_s+h_1}{a}\sqrt[3]{\frac{1-v_2{}^2}{1-v_e{}^2}}$$

(7.10) $$k = \sqrt[3]{\frac{E_s}{E_e}}$$

This model can be used to predict the settlement of a reinforced soil layer.

Poisson's ratio for the both styrofoam sheets was assumed to be 0.3, and from the above approach, the Young's modulus for the soil, thin styrofoam sheets, and the thick styrofoam sheets were found to be 7.42 MPa, 0.41 MPa, and 0.76 MPa, respectively. For an applied stress, the measured settlement for each geogrid case was determined from the load-settlement curves and the predicted settlement was calculated.

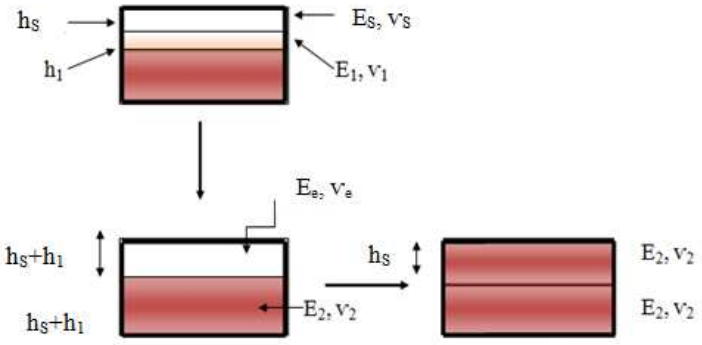

Figure 7.5 Layered elastic analysis (Vakili 2008).

Under 1G, the displacements were calculated and compared with the measured displacement under the same load. The results indicated that all of the measured displacements were at the same range with just 1 to 2 mm displacement different between unreinforced and reinforced soil. The results under 1G are presented in Table 7.2 and plotted in Figure 7.6.

Table 7.2 Measured and predicted footing settlements corresponding to an applied load under 1G

Layer depth	$q_{applied}$ (MPa)	h_1 (mm)	h_2 (mm)	ν_1	E_e (MPa)	ν_e	h_e (mm)	$W_{z,calc}$ (mm)	$W_{z,measured}$ (mm)
None	0.016	33	17	0.30	4.56	0.3	89.4	1.500	1.246
0.25B	0.016	33	17	0.30	4.56	0.3	89.4	1.500	1.365
0.5B	0.016	33	17	0.23	4.56	0.2	83.9	1.482	1.213
0.75B	0.016	33	17	0.23	4.56	0.3	85.5	1.487	1.213
1B	0.016	33	17	0.25	4.56	0.3	86.6	1.490	1.244
multi.	0.016	33	17	0.15	4.56	0.2	81.3	1.475	1.128

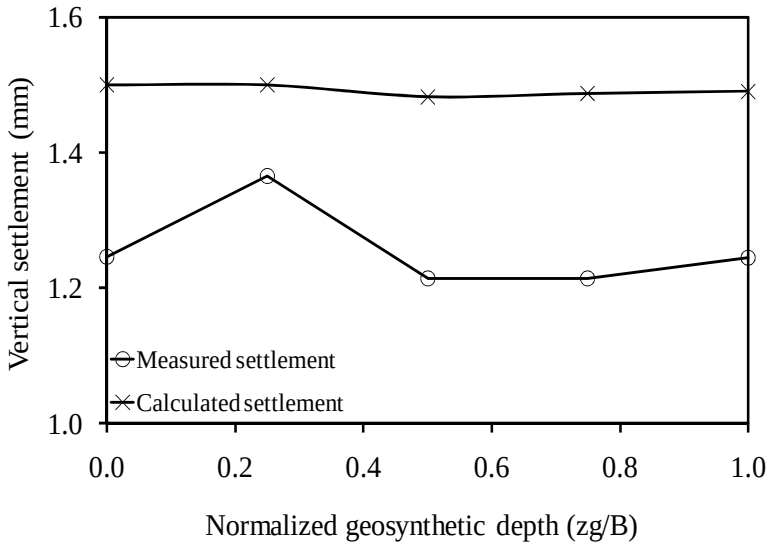

Figure 7.6 Calculated and measured settlements under 1G

The results under 20G indicate that the unreinforced soil and reinforced soil gave almost the same displacement. The results under 20G are presented in Table 7.3 and plotted in Figure 7.7. The Poisson's ratio of the reinforced granular fill was varied to result in an improved fit to the data. A smaller Poisson's ratio is intended to represent a soil layer with more lateral restraint.

Table 7.3 Measured and predicted displacement corresponding to an incorporated load - 20G

Layer depth	$q_{applied}$ (MPa)	h_1 (mm)	h_2 (mm)	ν_1	E_e (MPa)	ν_e	h_e (mm)	$W_{z,calc}$ (mm)	$W_{z,measured}$ (mm)
None	0.16	29	17	0.30	3.39	0.30	75.5	7.80	8.88
0.25B	0.16	29	17	0.10	3.39	0.16	66.7	7.66	6.94
0.5B	0.16	29	17	0.15	3.39	0.20	68.9	7.69	7.42
0.75B	0.16	29	17	0.12	3.39	0.17	67.6	7.67	7.12
1B	0.16	29	17	0.20	3.39	0.23	71.1	7.72	8.21
multi.	0.16	29	17	0.05	3.39	0.11	64.3	7.64	5.90

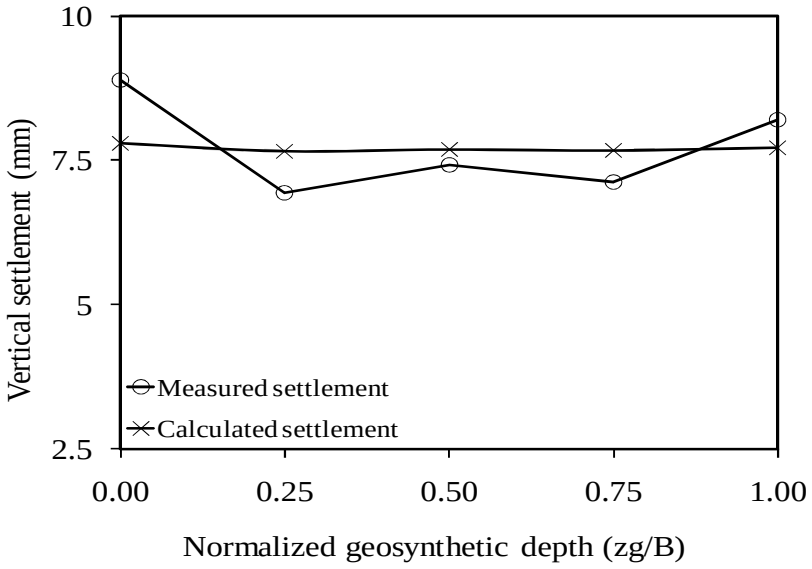

Figure 7.7 Calculated and measured settlements under 20G

The results under 40G are showing that the reinforced soil did not reduce the expected settlement, and the displacements from reinforced soil were the same as in the unreinforced soil. The results under 40G are presented in Table 7.4 and plotted in Figure 7.8.

Table 7.4 Measured and predicted displacement corresponding to an incorporated load - 40G

Layer depth	$q_{applied}$ (MPa)	h_1 (mm)	h_2 (mm)	ν_1	E_e (MPa)	ν_e	h_e (mm)	$W_{z,calc}$ (mm)	$W_{z,measured}$ (mm)
None	0.158	29	17	0.30	3.59	0.30	76.0	7.28	7.47
0.25B	0.158	29	17	0.20	3.59	0.23	71.5	7.21	6.23
0.5B	0.158	29	17	0.27	3.59	0.28	74.6	7.26	7.45
0.75B	0.158	29	17	0.25	3.59	0.27	73.7	7.24	7.16
1B	0.158	29	17	0.22	3.59	0.25	72.4	7.22	6.74
multi.	0.158	29	17	0.15	3.59	0.20	69.4	7.18	6.22

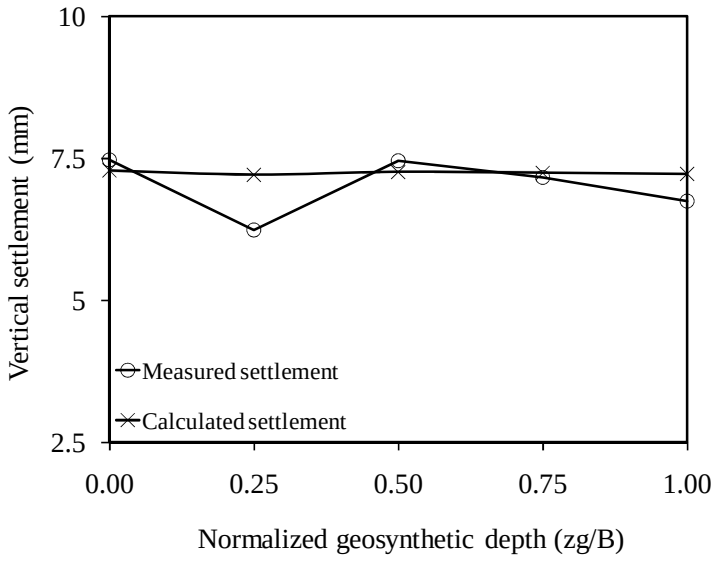

Figure 7.8 Calculated and measured settlements under 40G.

CHAPTER VIII

Conclusions

This study was performed to evaluate the impact of confining pressure on the pullout behavior of the geosynthetic reinforcement when placed at different depths under the centrifuge modeling. The centrifuge was found to be useful to evaluate the impact of soil self-weight on the impact of geosynthetic reinforcement on the load-settlement curves of granular fill overlying soft soils. The following specific conclusions can be drawn from this study are:

- Styrofoam sheets were found to be useful in modeling soft soils underlying a layer of granular fill.
- The centrifuge g-level was found to result in an increase in stiffness of the unreinforced soil layers under low levels of displacements. At high footing displacements, the g-level was found not to have an impact on the footing settlement.
- The geosynthetic reinforcement did not have a significant impact on the load settlement behavior of the foundations at low levels of displacement. However, at higher levels of displacement the load-settlement curves were found to be strongly dependent on the presence of the geogrid reinforcement. Geogrid reinforcements located closer to the foundation were found to lead to the stiffest load-settlement response.
- Modeling of models was used to check the validity of the scaling relations and to evaluate the impact of scale effects. A softer response was noted for foundations tested under higher g-levels. The results obtained from modeling of models indicted that there was no effect of the geogrid on the load-settlement curve.
- Future tests may benefit from using a soil having higher stiffness. Using material with higher stiffness will increase the interaction between the geosynthetic and the fill layer.

References

Abu-Farsakh, M.Y.; Qiming, C.; Radhey, S.; and Xiong, Z. (2008). "Large-Scale Model Footing Tests on Geogrid-Reinforced Foundation and Marginal Embankment Soils." Geotechnical Testing Journal, Vol. 31, pp. 413-423.

Aiban, S.A., and Znidarcic, D. (1995). "Centrifugal Modeling of Bearing Capacity of Shallow Foundation on Sands". Journal of Geotechnical Engineering , Vol. 121, pp. 1-10.

Brown, R.; Valsangkar, A. J.; Schriver, A.B. (2004). "Centrifuge modeling of surface footings on a sand layer underlain by a rigid base." Geotechnical and Geological Engineering, Vol. 12, pp. 187-198.

Boushehrian, A.H. and Hataf, N. (2008). "Bearing Capacity of Ring Footings on Reinforced Clay." 12th International Conference of International Association for Computer Methods and Advances in Geomechanics (IACMAG), Goa, India, pp. 3546-3551.

Bearden, J.B. and Labuz, J.F. (1998). "Fabric for Reinforcement and Separation in Unpaved Roads." Paul, Minnesota: Minnesota Department of Transportation.

Cerato, A.B. and Lutenegger, A.J. (2007). "Scale Effects of Shallow Foundation Bearing Capacity on Granular Material." Journal of Geotechnical and Geoenvironmental Engineering, Vol. 133, pp.1192-1202.

Das, B.M. (2009). "Shallow foundations Bearing Capacity and Settlement." Boca Raton, FL: Taylor and Francis Group.

Das, B.M., Shin, E.C., and Omar, M.T. (1994)."The Bearing Capacity of Surface Strip Foundations on Geogrid Reinforced Sand and Clay". Geotechnical and Geological Engineering , Vol. 12, pp. 1-14.

Dash, S.K.; Rajagopal, K. ; and Krishnaswamy, N.R. (2004). "Performance of Different Geosynthetic Reinforcement Materials In Sand Foundations." Geosynthetics International, Journal of International Geosynthetics Society, Vol. 11, pp. 35-42.

Dash, S.K.; Sieesh, S.; and Sitharam,T.G. (2003). "Behaviour of geocell-reinforced sand beds under circular footing." Ground Improvement, Journal of International Society of Soil mechanics and Geotechnical Engineering Vol. 7, pp. 111-115.

DeMerchant, M.R.; Valsangkar, A.J.; and Schriver, A.B. (2002). "Plate Load Tests on Geogrid Reinforced Expanded Shale Lightweight Aggregates." Geotextiles and Geomembranes. Vol. 20, pp. 173-190.

Department of the Army U.S. Army Corps of Engineers. (1992). "Engineering and Design Bearing Capacity of Soils." Department of the Army U.S. Army Corps of Engineers. Vol. 196.

Dong, Y.L.; Han, J.; Qian, Y.; and Bai, X.H. (2010). "Behavior of triangular aperture geogrid-reinforced bases under static loading". 9th International Conference on Geosynthetics, Brazil , pp 1547-1550.

Fellenius, B.H. and Altaee, A. (1994)."Stress and Settlement of Footings In Sand." Conference on Vertical and Horizontal Deformations for Foundations and Embankments, Geotechnical Special Publication, GSP, No. 40, College Station, TX, Vol. 2, pp 1760-1773.

Gabr, M.A. and Hart, J.H. (2000). "Elastic Modulus of Geogrid- Reinforced Sand Using Plate Load Tests." Geotechnical Testing Journal, ASTM, Vol. 23, pp. 245-250.

Giroud, J.P., and Han, J. (2004). "Design Method for Geogrid-Reinforced Unpaved Roads. I. Development of Design Method." Journal of Geotechnical and Geoenvironmental Engineering, Vol. 130, pp. 775-786.

Guler, E.; Yetimoglu, T.; and Cicek, E. (2010). "Bearing capacity of shallow foundations on reinforced clay soil." 9th International Conference on Geosynthetics. pp.1989-1992, Brazil.

Ismail, I. and Raymond, G.P. (1995). "Geosynthetic Reinforcement of Granular Layered Soils." Geosynthetics '95, pp.317-330.

Ko, H.Y. (1988), “Summary of the state-of-the-art in centrifuge model testing.”, Centrifuge in Soil Mechanics, Craig, James, and Schofield, eds., Balkema Publishers, The Netherlands, pp. 11-18.

Kumar, A. and Walia, B.S. (2006). "Bearing capacity of square footings on reinforced layered soil." Geotechnical and Geological Engineering. Vol. 21, pp. 201-224.

Lee, Y-B. (2010). "Deformation Behavior of Shored Mechanically Stabilized Earth Walls." PhD dissertation, U. of Colorado at Boulder.

McCartney, J.S; Cox, B.R.; Wood, C.M.; and Curry, B.(2004). "Evaluation of Geosynthetic-Reinforced Flexible Pavements Using Static Plate Load Tests." 9th IGS Conference. Guaruja, Brazil. Vol. 3, pp. 1445-1450.

Marandi, S.M.; Bagheripour, M.H.; Rahgozar, R.; and Ghirian, A.R. (2008). "Numerical Investigation Into The Behavior of Circular Pad Shallow Foundations Supported By Geogrid Reinforced Sand." American Journal of Applied Sciences, Vol. 5, pp. 355-368.

Michalowski, R.L. (2004). "Limit Loads on Reinforced Foundation Soils." Journal of Geotechnical and Geoenvironmental Engineering, Vol. 130, pp. 381-390.

Murthy, V.S. (2002). "Geotechnical Engineering: Principles and Practices of Soil Mechanics and Foundation Engineering". New York: Marcel Dekker.

Vakili, J. (2008). “A Simplified Method for Evaluation of Pavement Layers Moduli Using Surface Deflection Data.” The 12th Int. Conf. of Int. Assoc. for Comp. Methods and Adv. In Geomechanics (IACMAG). 1-6 Oct. Goa, India.

Winterkorn, H.F. and Fang, H. (1975). "Foundation Engineering Handbook." New York: Van Nostrand Reinhold Company Inc.